Overview of the CPOC Pilot Study at Whiteface Mountain, NY
Cloud Processing of Organics within Clouds (CPOC)

Photo taken September 2017 by Carl Heilman II

Sara Lance, Jie Zhang, James J. Schwab, Paul Casson, Richard E. Brandt, David R. Fitzjarrald, Margaret J. Schwab, John Sicker, Cheng-Hsuan Lu, Sheng-Po Chen, Jeongran Yun, Jeffrey M. Freedman, Bhupal Shrestha, Qilong Min, Mark Beauharnois, Brian Crandall, Everette Joseph, Matthew J. Brewer, Justin R. Minder, Daniel Orlowski, Amy Christiansen, Annmarie G. Carlton, and Mary C. Barth

ABSTRACT: Aqueous chemical processing within cloud and fog water is thought to be a key process in the production and transformation of secondary organic aerosol mass, found abundantly and ubiquitously throughout the troposphere. Yet, significant uncertainty remains regarding the organic chemical reactions taking place within clouds and the conditions under which those reactions occur, owing to the wide variety of organic compounds and their evolution under highly variable conditions when cycled through clouds. Continuous observations from a fixed remote site like Whiteface Mountain (WFM) in New York State and other mountaintop sites have been used to unravel complex multiphase interactions in the past, particularly the conversion of gas-phase emissions of SO_2 to sulfuric acid within cloud droplets in the presence of sunlight. These scientific insights led to successful control strategies that reduced aerosol sulfate and cloud water acidity substantially over the following decades. This paper provides an overview of observations obtained during a pilot study that took place at WFM in August 2017 aimed at obtaining a better understanding of Chemical Processing of Organic Compounds within Clouds (CPOC). During the CPOC pilot study, aerosol cloud activation efficiency, particle size distribution, and chemical composition measurements were obtained below-cloud for comparison to routine observations at WFM, including cloud water composition and reactive trace gases. Additional instruments deployed for the CPOC pilot study included a Doppler lidar, sun photometer, and radiosondes to assist in evaluating the meteorological context for the below-cloud and summit observations.

AFFILIATIONS: **Lance, Zhang, J. Schwab, Casson, Brandt, Fitzjarrald, Schwab, Sicker, Lu, Chen,* Yun,* Freedman, Shrestha, Min, Beauharnois, Crandall,* and Joseph***—Atmospheric Sciences Research Center, University at Albany, State University of New York, Albany, New York; **Brewer* and Minder**—Department of Atmospheric and Environmental Sciences, University at Albany, State University of New York, Albany, New York; **Orlowski***—Rensselaer Polytechnic Institute, Troy, New York; **Christiansen and Carlton**—University of California, Irvine, Irvine, California; **Barth**—National Center for Atmospheric Research, Boulder, Colorado

* CURRENT AFFILIATIONS: Chen—Center for Environmental Studies, National Central University, Taiyuan, Taiwan; **Yun and Crandall**—New York State Department of Environmental Conservation, Albany, New York; **Joseph**—National Center for Atmospheric Research, Boulder, Colorado; **Brewer**—San Jose State University, San Jose, California; **Orlowski**—New York City Department of Environmental Protection, New York, New York

Atmospheric pollution can have significant impacts on human and ecosystem health, visibility, and climate (NAS 2016; Seinfeld and Pandis 2016). Control strategies require knowledge of the chemical and physical transformations that pollutants undergo as they are transported downwind of emission sources. Cloud water plays an important role in the transformation of atmospheric pollutants, including removal of pollutants from the atmosphere via wet deposition and scavenging of gases and aerosols that can participate in aqueous chemical reactions within cloud droplets (Ervens et al. 2011, 2013; McNeill 2015).

Whiteface Mountain (WFM), one of the highest peaks in the Adirondack Mountains in the northern part of New York State, has a long history of reactive trace gas and cloud water chemical measurements (Schwab et al. 2016a,b; Brandt et al. 2016). The isolated peak of WFM sits at an altitude of 1,483 m, while summertime cloud-base height in this region typically sit at 1,100 m, resulting in clouds intercepting the summit 20%–60% of the time throughout

AMERICAN METEOROLOGICAL SOCIETY   BAMS   OCTOBER 2020   **E1821**

Unauthenticated | Downloaded 05/27/22 08:09 PM UTC

the summer months (Schwab et al. 2016a), making WFM an excellent location for long-term studies of aerosol–cloud interaction processes.

A remote location such as WFM represents regional background conditions, generally signifying the best air quality that a city within the nearby region can hope to achieve (e.g., Rattigan et al. 2016). Air quality in both urban and rural locations across the United States has improved steadily over the past several decades in response to implementation of federal and regional air quality standards (Hand et al. 2012; Lin et al. 2017; Civerolo et al. 2017). In particular, regulations have steadily reduced fine particulate matter (PM_1), especially in the eastern United States, largely through reductions in sulfate aerosol (Rattigan et al. 2017; Blanchard et al. 2019). Multiphase chemistry observations at the summit of WFM and other mountain sites beginning in the 1970s helped to establish a dominant reaction pathway for secondary sulfate formation from gas-phase SO_2 emissions within cloud droplets in the presence of sunlight (Falconer and Falconer 1980; Möhnen and Kadlecek 1989; Husain 1989; Husain and Dutkiewicz 1990; Möhnen and Vong 1993), and these seminal observations provided the scientific evidence definitively linking SO_2 emissions to acid rain. Nearly all cloud water monitoring programs in the northeastern United States [e.g., some of which were highlighted by Weathers et al. (1988) and Anderson et al. (1999)] have subsequently been discontinued since the acid rain problem has been "solved," and the multi-decades-long cloud water monitoring program at WFM (supported by the State of New York) was gradually cut back from hourly sampling to 3-hourly sampling in 2007 to 12-hourly sampling in 2014 to reduce costs associated with site visits and chemical analysis.

Meanwhile, cloud chemistry research has experienced a resurgence in scientific interest due to the potential for aqueous chemical processes to help fill the gap between modeled and observed organic aerosol mass (Kanakidou et al. 2005; Heald et al. 2005; Volkamer et al. 2006; Ervens 2015; Herrmann et al. 2015) and the ubiquity of organic aerosol in recent years, which is largely thought to be secondary organic aerosol (SOA) produced in the atmosphere from gas-phase precursors (Zhang et al. 2007). A wide array of natural and anthropogenic emissions can play a role in SOA formation. While analogies can be made between inorganic and organic chemical processing in clouds (Gelencsér and Varga 2005), organics are considerably more complex (Saxena and Hildemann 1996; Samburova et al. 2013; Ehn et al. 2014; Hunter et al. 2017; X. Zhang et al. 2017; Lee et al. 2018; Ditto et al. 2018), even in the simplest of cases [e.g., starting with a single volatile organic compound and a single gas-phase oxidant, as in Carlton et al. (2007)]. Chemical aging of organics in the atmosphere can include functionalization, fragmentation, and/or oligomerization reactions that can impact the chemical properties of the organic compounds in different ways (Jimenez et al. 2009; Yu et al. 2016; Huang et al. 2018), and the evolution of individual organic compounds often takes place over multiple reaction steps (Carlton et al. 2009; Isaacman-VanWertz et al. 2018). The resulting changes to the hygroscopicity and volatility of organic compounds in the atmosphere impact the particle size distribution and atmospheric lifetime of aerosols, with implications for visibility, climate and human health (Hallquist et al. 2009; Farmer et al. 2015; Ridley et al. 2018). The specific chemical properties of the SOA formed may also factor in to their impact on health (Tong et al. 2017; Chowdhury et al. 2018; Rich et al. 2019). As organics become an ever larger fraction of atmospheric pollutants, it is increasingly important to understand their sources, detailed composition, transformation, and fate (Herckes et al. 2013).

The purpose of this paper is to highlight results from the Chemical Processing of Organic Compounds within Clouds (CPOC) pilot study that took place in August 2017 at WFM and evaluate the WFM summit research observatory as a platform for tackling the complex problems associated with measuring chemical processing of organics within clouds, as outlined during the 2016 National Science Foundation–funded Cloud Water Chemistry workshop that

took place at WFM in 2016 (Lance et al. 2017). A more basic and pressing goal for the CPOC pilot study was for current researchers at the University at Albany's Atmospheric Sciences Research Center (ASRC) to obtain hands-on experience and transfer of knowledge from previous principal investigators (PIs) in regard to cloud water collection protocols before the ongoing long-term cloud monitoring measurement contract ended in 2017.

Methods

Field sites. The ASRC at the University at Albany operates two long-term measurement sites at WFM: a four-story research observatory at the summit and a lodge facility site (600 m elevation), labeled as Summit and Lodge in Fig. 1. A wide variety of trace gas, aerosol, and meteorological measurements have been carried out for decades at these two sites (Brandt et al. 2016; Schwab et al. 2016a), and cloud water sampling has been conducted at the summit (Schwab et al. 2016b). The WFM summit research observatory is above the tree line, and the predominant winds out of the west provide an unobstructed alpine fetch that is largely unperturbed by local anthropogenic sources upwind of the site, with the ski area on the downwind eastern slopes.

Key additional instruments were deployed at three primary locations for the CPOC field project: 1) the WFM summit research observatory (1,483 m elevation), 2) the Lake Placid Turn (LPT) alongside the Whiteface Memorial Highway (1,249 m elevation), and 3) Northwood School in the town of Lake Placid (584 m elevation) (Fig. 1). Photographs of the sites are shown in Fig. 2.
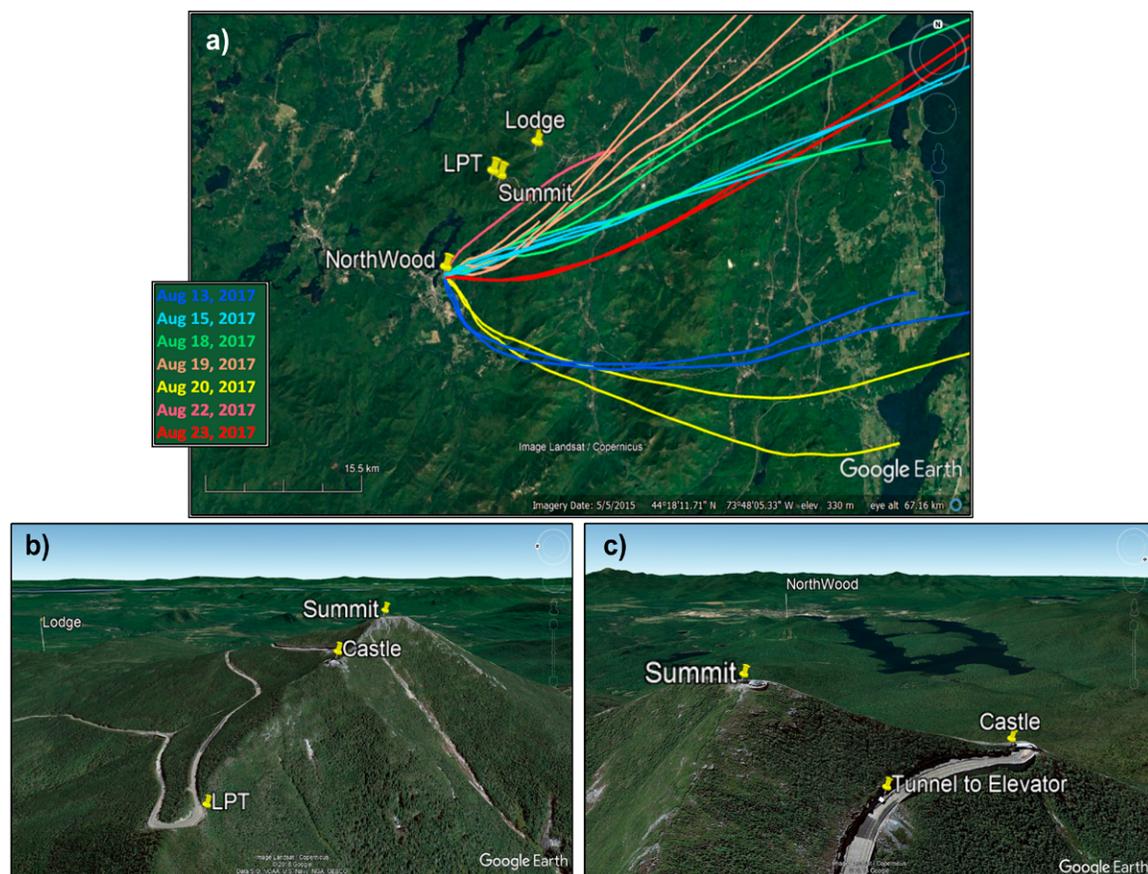

Fig. 1. (a) Trajectories of the balloon launches out of Northwood School colored by day, and two different Google Earth views of the summit, facing (b) due east and (c) southwest. The Lake Placid Turn, so named because it is a sharp turn in the road facing Lake Placid, is labeled in (a) and (b) as LPT, where the ASRC Sprinter van was deployed during the CPOC pilot study. The castle indicated in (b) and (c) is the highest point on the mountain reachable by car. For heavy equipment access to the summit, tunnel access to the elevator must be used, as indicated in (c).

The LPT was chosen as the below-cloud measurement site, as it is the lowest point along the ridgeline to the summit accessible by car, where it can receive air directly from the southwestern quadrant, generally upwind of WFM.

Northwood School provided the needed infrastructure for power, Internet, and accessibility for a site <10 km upwind of WFM. The remote sensing and balloon-borne measurements deployed/launched from Northwood School were used to obtain vertical profiles of winds, aerosols, clouds, and other meteorological conditions in the vicinity of WFM during time periods of special interest, which generally corresponded to time periods when the ASRC Sprinter van was deployed below-cloud at the LPT while the summit was in-cloud. Radiosondes launched at Northwood School caught the predominant winds and were carried as far east as Lake Champlain on the border between New York and Vermont (Fig. 1a).

Measurements. Routine cloud water chemical monitoring at WFM began in 1994 with the Mountain Acid Deposition Program (Baumgardner et al. 2003) and continued under the stewardship of the Adirondack Lake Survey Corporation (ALSC) (Dukett et al. 2011; Aleksic et al. 2009) until 2017, yielding a continuous long-term record of summertime liquid water content (LWC), bulk cloud water pH, conductivity, sulfate SO_4^{2-}, nitrate NO_3^-, ammonium (NH_4^+), potassium (K^+), chloride (Cl^-), sodium (Na^+), calcium (Ca^{2+}), and magnesium (Mg^{2+}). Total organic carbon (TOC) was added to these routine summer measurements
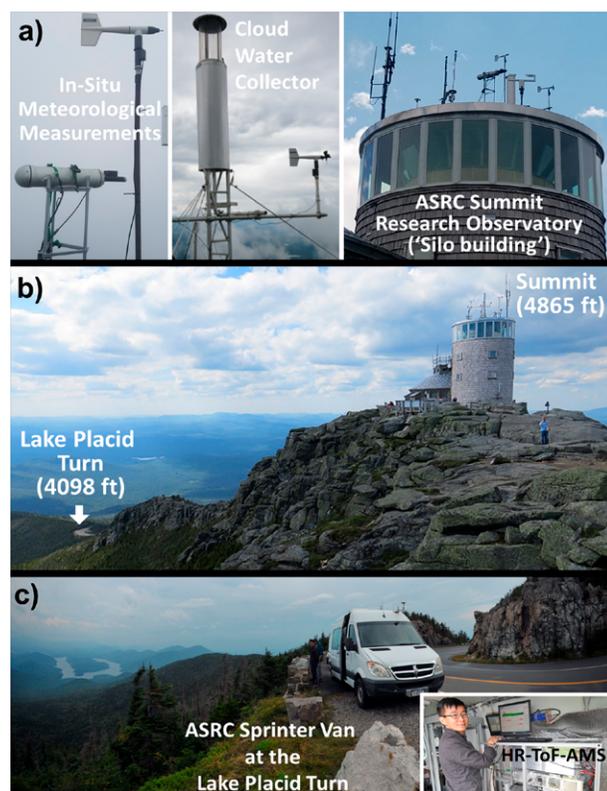

Fig. 2. Photographs showing key aspects of the CPOC pilot study: (a) in situ meteorological observations on the roof of the ASRC summit research observatory, (b) the relative locations of two primary measurement locations during the CPOC pilot study (the LPT and the summit) and their respective altitudes, and (c) a close-up view of the ASRC Sprinter van at the LPT, with unobstructed view of Lake Placid in the distance, and the HR-ToF-AMS deployed from the Sprinter van (inset shows Jie Zhang, who operated the HR-ToF-AMS during CPOC).

starting in 2009. In previous cloud water studies, TOC has been found to be dominated by soluble material, with a ratio of dissolved organic carbon (DOC) to TOC in the range of 0.77–0.94 (Herckes et al. 2013) for cloud water collected at several other locations. For this entire long-term record, the same basic equipment and protocols were used, including a Möhnen omnidirectional passive cloud water collector (Möhnen and Kadlecek 1989) and a Gerber Particulate Volume Monitor (PVM) (Gerber 1991). Cloud water collection commences when the following conditions are met: 1) LWC as measured by the Gerber PVM exceeds 0.05 g m⁻³, 2) wind speed as measured by an RM Young anemometer exceeds 2 m s⁻¹, 3) temperature exceeds 2°C, and 4) no rain is detected. Since 2015, a Canadian Acid Precipitation Monitoring Network (CAPMoN) capacitive rain sensor (Mekis et al. 2018) has been used to indicate whether or not it is raining/drizzling.

In 2017, diurnal (12 hourly, i.e., one nighttime and one daytime sample per day) cloud water sampling was conducted by ALSC at the summit of WFM as per their long-term contract with State of New York. In addition, since large volumes of cloud water are frequently obtained at WFM in excess of the 250 mL needed by ALSC to conduct their routine chemical analyses, during the CPOC pilot study excess cloud water was set aside for measurement of additional chemical compounds via other measurement methods. Furthermore, during select time periods, hourly cloud water sampling was conducted, whereby each hourly sample was weighed and divided

equally into two aliquots. One of these aliquots was set aside for additional analysis while the other was combined with other samples for each 12-h period. This protocol enabled both the 12-hourly sampling required by ALSC while also allowing for additional chemical analysis at higher time resolution, using only one cloud water collector.

A summary of the instruments deployed during the CPOC pilot study and their deployment location is given in Table 1. Of the instruments not normally deployed at WFM, the High Resolution Time of Flight Mass Spectrometer (HR-ToF-AMS) (Drewnick et al. 2005) provided measurements of highest scientific value for the CPOC pilot study, because real-time measurements of dry aerosol chemical composition are fundamental to the study of chemical processing of aerosols in-cloud. Other important instruments deployed during CPOC included two sets of nearly identical instruments at the summit and at the LPT, including a cloud condensation nuclei counter (CCNc; DMT CCN-100) (Lance et al. 2006; Rose et al. 2008) and a scanning mobility particle sizer (SMPS), as illustrated in Fig. 3, which provided additional information about the aerosol microphysical properties. Both SMPS systems used the same long column differential mobility analyzer (DMA; TSI 3081), but out of necessity the SMPS at the summit used a butanol CPC (TSI 3022 A) and the SMPS in the ASRC Sprinter van used a water-based CPC (TSI 3785). Since measurements obtained at the LPT during the CPOC pilot study have been reported by Zhang et al. (2019), this paper focuses on measurements obtained from the WFM summit.

During the pilot study, a Fast-Forward Scattering Spectrometer Probe (FFSSP) was operated at WFM for the first time to obtain the cloud droplet size distribution. This particular instrument still has the original tubular inlet with a blower mounted to the back of it, which pulls air through the inlet to enable ground-based operation under low wind speed conditions (e.g., radiative fogs). The strong winds typically encountered at the summit of WFM require active orientation of the FFSSP into the wind to ensure that droplets transit straight through the instrument sample area within the inlet tube. Thus, a motorized rotating platform was built for the FFSSP (Fig. 4). This motorized

Table 1. List of instruments deployed during the CPOC pilot study and their deployment location. Routine long-term measurements at WFM are described in a series of papers published in 2016 (Schwab et al. 2016a,b; Brandt et al. 2016) and are not included here. During CPOC, a meteorological (met) tower and tipping-bucket rain gauge were also deployed on the roof of the "castle" (at 1,402 m elevation, Fig. 1).

| Location	Instruments
WFM summit	Inside the Silo building: CCNc, SMPS
	On the roof of the Silo building: FFSSP, disdrometer, tipping-bucket rain gauge
Lake Placid Turn	ASRC Sprinter van: CCNc, SMPS, CPC, HR-ToF-AMS
	Free-standing met tower: humidity, temperature, wind direction and speed, solar radiation
Northwood School	Balloon-borne radiosondes, Doppler lidar, sun photometer

a)

b)
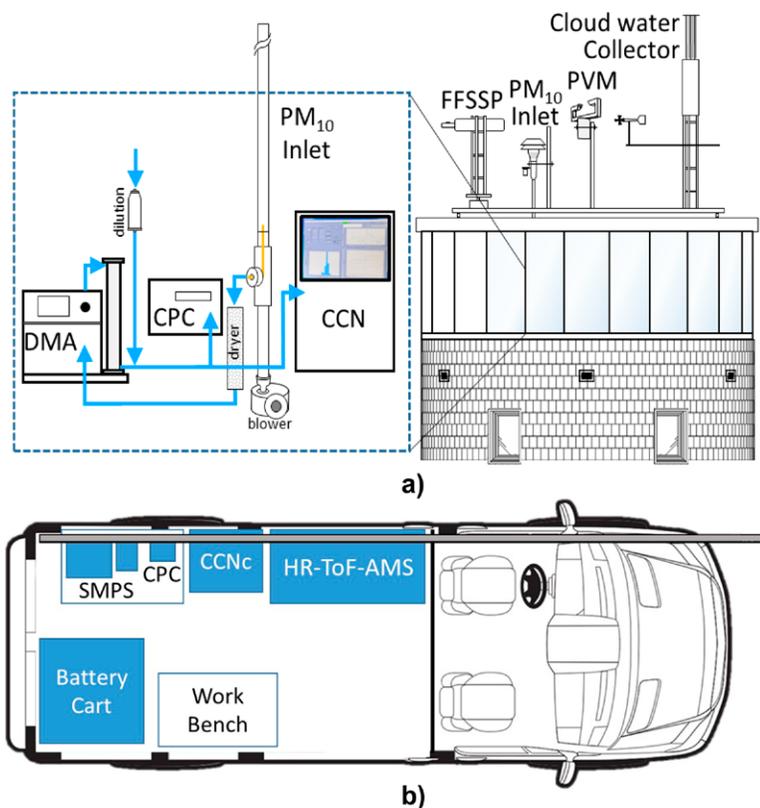
Fig. 3. (a) Instruments and inlets on the roof of the ASRC summit research observatory (also known as the Silo building) and housed within the top floor of the Silo building during the CPOC pilot study. (b) Instruments housed within the ASRC Sprinter van.

stage included a heavy-duty turntable (designed for a sand-blasting cabinet), motorcycle gear set, waterproof stepper motor, RM Young wind vane, and Arduino microprocessor. The program controlling the FFSSP orientation read the wind direction continually, driving the stepper motor every 5 min and returning back to the starting position prior to each new position change to prevent the power supply and communications cables from getting
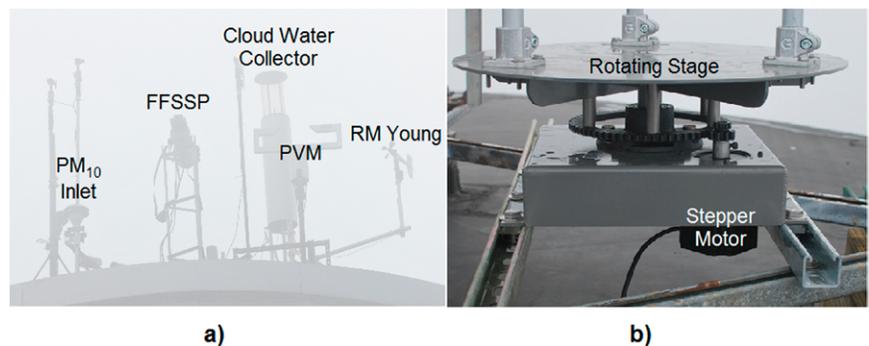

Fig. 4. Photographs of (a) instruments on the roof of the Silo building while sampling clouds during CPOC, as viewed from just outside the base of the Silo building on the upwind side, and (b) the base of the FFSSP tower on the roof of the Silo building, attached to a rotating stage, driven by a stepper motor.

entangled. The CPOC pilot study was also the first deployment of the FFSSP after updating with modern "Fast" electronics. This was a significant upgrade to the original FSSP electronics, which suffered from severe electronic dead time. The additional information acquired about every particle passing through the FFSSP laser beam allows for the ability to better characterize and accurately account for "coincidence" errors on the measured droplet size distribution. However, there are drawbacks to the electronics upgrade: continuous sampling night and day at a ground-based site can be a challenge for internal memory storage and data transfer, especially given the high frequency of cloud events at the summit of WFM. The FFSSP sizing response and sample area were calibrated by the company that performed the electronics upgrade (SPEC, Inc.), using a standardized water droplet calibration system (Lance et al. 2010).

The Gerber PVM probe has been used for many years at the summit of WFM as a measurement input for the cloud water collection system. Operating the FFSSP side by side with the Gerber PVM during the CPOC pilot study provided the opportunity to evaluate the LWC values derived from the PVM measurements. While the PVM is generally used only to evaluate whether or not a cloud is present, the long-term LWC measurements obtained by the PVM can be useful for calculating cloud water mass loadings for direct comparison to aerosol mass loadings, if the accuracy of the cloud LWC measurements can be relied upon.

A Doppler lidar (Leosphere WindCube) and environmental Sky Imager-Radiometer (eSIR) (Yin et al. 2011) were also deployed at the Northwood School. Radiosondes launched from the site were fitted with iMet-1 sensors (International Met Systems, Inc.).

Logistics and measurement strategy during the CPOC pilot study. The CPOC pilot study took place 12–23 August 2017. Supplemental instruments deployed during the study (as described above) were provided by researchers at the University at Albany, and the field work was largely supported by a handful of students. During the pilot study, a minimum of three people were needed to fulfill the day-to-day operations: 1) one person stationed at the summit to obtain hourly cloud water samples, 2) one person to launch radiosondes from Northwood School, and 3) one person to drive the ASRC Sprinter van to the LPT and obtain below-cloud aerosol measurements. The measurement strategy targeted situations when the WFM summit was in-cloud and the LPT was below-cloud, largely to compare the below-cloud aerosol composition and the cloud water composition to assess the impact of cloud processing on the aerosol chemical composition. Cloud and aerosol microphysical measurements at the summit provided further information about the sampling conditions and aerosol–cloud interactions.

The ASRC Sprinter van was deployed to the LPT for up to 4 h at a time, depending on the power draw on the batteries, largely controlled by the instrument payload and the need for air conditioning. Only daytime deployments, when the LPT was likely to be below cloud base, were undertaken. After each deployment, the Sprinter van was returned to the WFM lodge to recharge.

The CCNc and SMPS were installed at the summit early in the summer, and parallel measurements were obtained starting on 22 June. Unfortunately, early in August the SMPS sheath blower failed and needed to be replaced, and particle size distribution measurements did not resume at the summit until 16 August. After this point, during the pilot study, size-resolved CCN measurements were obtained by operating the CCNc behind the DMA (in parallel with the CPC), which enabled aerosol hygroscopicity to be determined (Petters and Kreidenweis 2007; Moore et al. 2010). For both size-resolved CCN measurements and total CCN measurements, the CCNc supersaturation (SS) was cycled through five settings ranging from 0.23% to 0.78% (as calibrated), with 10 min given at each SS setting, except for the lowest SS setting (which was given 20 min to allow for thermal equilibration following the large change in temperature imposed).

Results

Summit observations. Figure 5 highlights several interesting observations made at the WFM summit during the summer of 2017, and provides context for the observations made during the CPOC pilot study (outlined with dotted lines). Cloud LWC (as measured by the Gerber PVM) was as high as 2.5 g m^{-3} in 2017, but generally remained below 1.5 g m^{-3} during the pilot study,
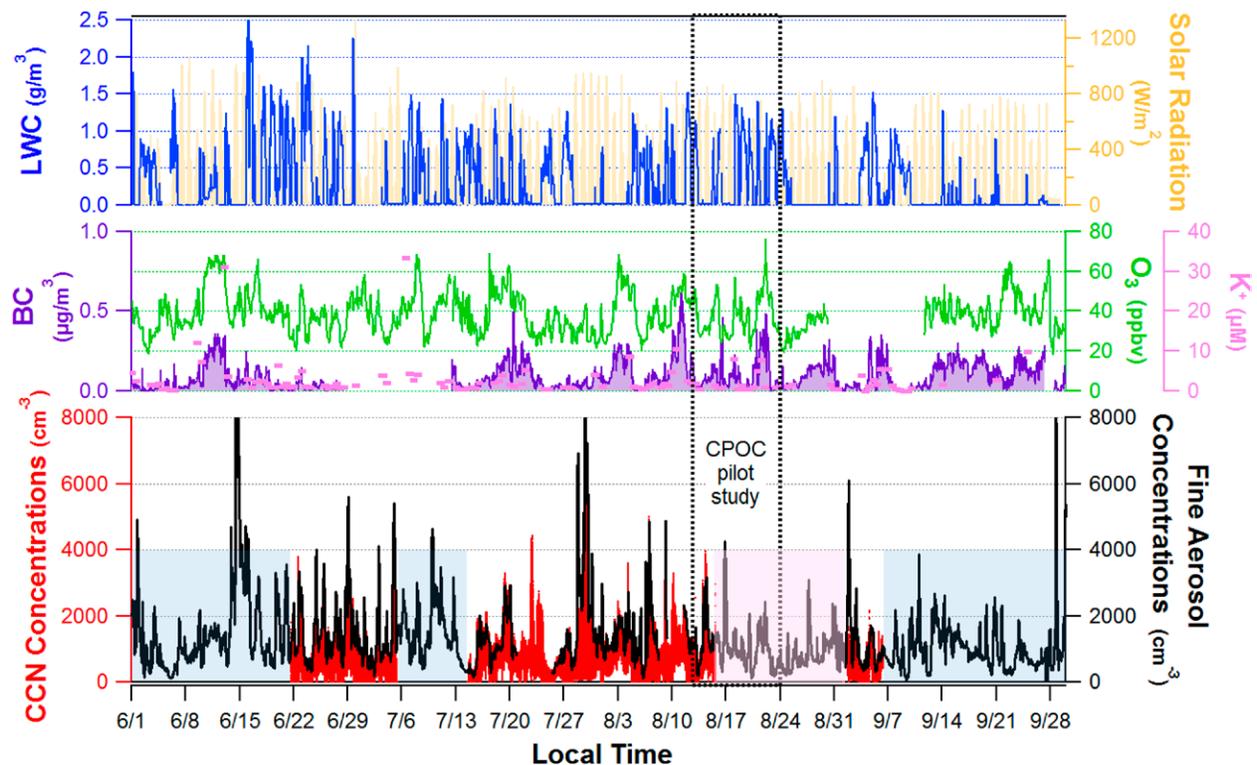

Fig. 5. WFM summit observations obtained throughout the summer of 2017, with the time period of the CPOC pilot study outlined with dotted lines. CCN measurements (indicated by the red trace) were size-resolved (as indicated by pink shaded region) during the CPOC pilot study and for the following week, but were not size-resolved for the remainder of the summer. When CCN measurements were not obtained, the time period is shaded blue. Cloud water potassium (K$^+$) concentrations (pink markers), indicative of biomass-burning plumes, were often correlated with enhancements in black carbon (BC) and ozone (O$_3$) concentrations (as indicated by the purple and green traces, respectively).

which was more typical for clouds intercepted in July and August. Episodes of relatively high black carbon (BC) mass concentrations (exceeding 250 ng m^{-3}) were observed throughout the summer and typically remained elevated for more than one day, and at least one of these episodes was captured during the pilot study. Elevated cloud water K$^+$ concentrations were also observed during the pilot study, generally corresponding to time periods with elevated BC. Cook et al. (2017) found that cloud water K$^+$ concentrations exceeded 1 μM in aged biomass burning plumes at WFM in August 2014. During CPOC, nearly half of the 12-hourly cloud water samples (33 out of 72) had K$^+$ concentrations exceeding 1 μM, suggesting that biomass burning was a significant driver for cloud water chemistry at WFM throughout the summer of 2017. In addition, ozone (O$_3$) concentrations tended to be elevated (>39 ppb) in air masses with elevated BC and cloud water K$^+$ concentrations, suggesting a common influence. Fine aerosol number concentrations averaged 1,200 cm^{-3} and CCN concentrations were 690 and 870 cm^{-3} (at 0.51% and 0.78% SS, respectively) throughout the summer, and neither were especially high during the CPOC pilot study.

Focusing on the time period of the CPOC pilot study (Fig. 6), LWC observations indicate that clouds more frequently intercept the summit of WFM during the nighttime hours (as indicated by solar radiation measurements, plotted in orange) and cloud base typically lifts in the morning, surpassing the summit by midday. This scenario characterized all but three days during the pilot study: 14 and 17 August (for which the summit was clear all day) and 19 August (for which the summit was cloudy for most of the day). Time periods in cloud are highlighted in blue in Fig. 6, and the dry aerosol particle size distribution suggests that during these time periods particles >~100 nm (and sometimes as small as 50 nm) were lost from the sample stream prior to the SMPS measurement. This dramatic reduction in the concentration of accumulation mode particles in-cloud indicates that cloud droplets typically exceeded 10 μm in diameter and could not pass through the PM$_{10}$ aerosol inlet. Therefore, the in-cloud aerosol measurements obtained at the WFM summit represent interstitial aerosol particles (and possibly cloud droplet residuals under conditions with low LWC and therefore relatively small droplets).
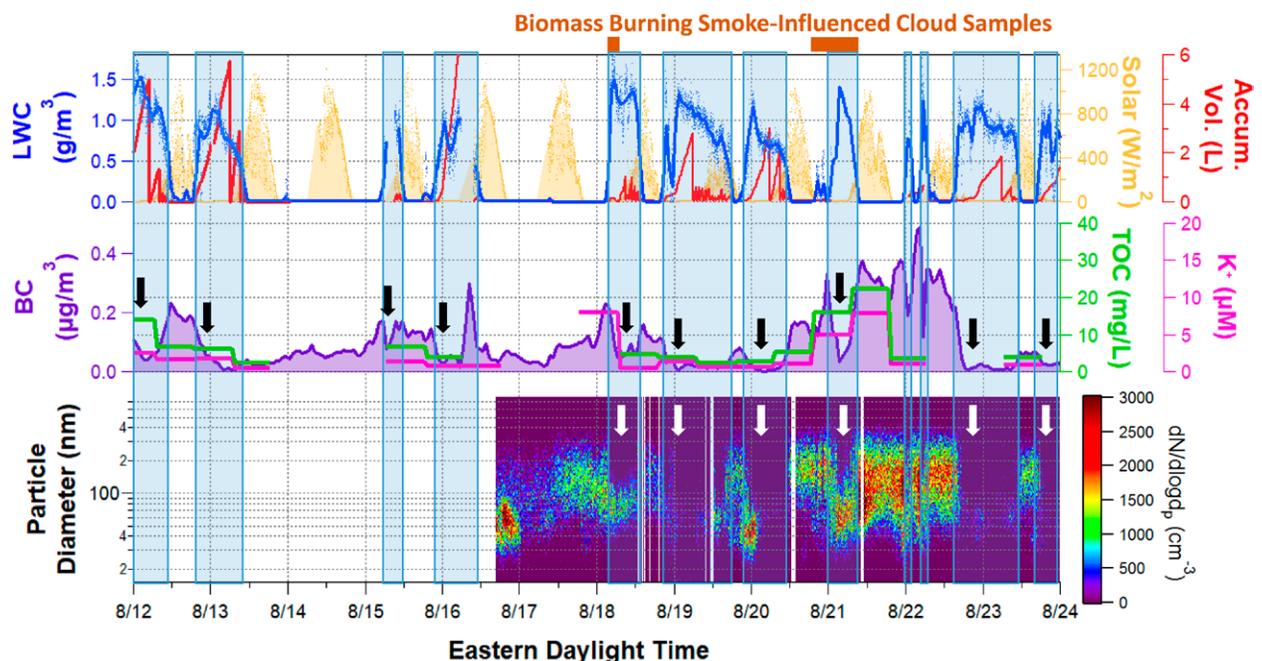

Fig. 6. Aerosol and cloud observations from the WFM summit during the CPOC pilot study. Time periods in-cloud are highlighted in blue. The caption in Fig. 5 applies again here, except that the green trace represents TOC and the red trace represents the accumulated cloud water volume. The dry particle size distribution is also shown.

These observations also suggest that BC was efficiently wet scavenged, which is especially clear on 21 August, with a marked anticorrelation between BC concentrations and cloud LWC (Fig. 6). The concurrent rapid decrease in BC mass (as highlighted in Fig. 6 by black arrows) and removal of particles >~100 nm (as highlighted with white arrows) suggest that particles acting as CCN were internally mixed with BC. Also shown in Fig. 6 are cloud water concentrations of TOC and K^+. Three 12-hourly cloud water samples during the CPOC pilot study had especially high K^+ concentrations (>5 μM), indicating wet scavenging of biomass burning smoke. Two of these cloud water samples were collected back to back on the morning of 21 August, and these two samples also exhibited the highest TOC during the pilot study (>15 mg C L^{-1}). Satellite observations show absorbing aerosols drifting over WFM on this day, as shown by Zhang et al. (2019). For comparison, TOC measurements in cloud water samples obtained at WFM in 2014 that were impacted by wildfire smoke ranged from 7.86 to 16.6 mg C L^{-1} (Cook et al. 2017). These concentrations are relatively low compared to TOC concentration reported for cloud water samples impacted by regional biomass burning smoke at a remote mountain site in China (100–200 mg C L^{-1}), some of the highest concentrations reported in a review paper of organics in fog and cloud water by Herckes et al. (2013). Cloud droplet size has also been found to be an important factor, with droplets >15 μm often having significantly lower TOC concentrations (Herckes et al. 2013). The cloud water sample collected in the early morning of 18 August corresponding to the highest K^+ of the study did not have enough volume for TOC analysis, but this was likely another episode of wet scavenged biomass burning smoke that intercepted the summit of WFM. Black carbon concentrations observed at the summit just prior to the summit becoming engulfed in clouds were also relatively high (>200 ng m^{-3}). An abrupt loss of particles >100 nm in the dry particle size distribution and abrupt reduction in BC occurred after clouds intercepted the summit on 18 August, and these reductions were sustained for the duration of the in-cloud sampling until midday, which again suggests that particles >100 nm acted as CCN and could no longer be sampled through the aerosol inlet, and that these CCN also comprised a significant fraction of the BC aerosol mass.

Fig. 7. Five-day ensemble back trajectories calculated using the HYSPLIT model, with the end location at the Lake Placid Turn.

Five-day back trajectory analysis (Fig. 7) using the HYSPLIT model (Stein et al. 2015; Draxler and Hess 1998) indicates transport from western Canada to WFM on 21 August. Smoke from major wildfires in British Columbia, which reportedly began on 6 July and burned until mid-September 2017, was observed across the United States and Canada and into the Arctic (Laing and Jaffe 2019; Lutsch et al. 2019), and occasionally injected into the lower stratosphere (Torres et al. 2018; Das et al. 2018; Chen et al. 2018).

In-cloud and clear air CCN concentrations from the morning of 13 August are shown in Fig. 8, prior to implementation of size-resolved CCN measurements. In addition to the previously noted loss of >~100 nm particles, time periods in-cloud are marked by significant reductions in the CCN-active fraction, as indicated by a gap between the fine aerosol concentrations in black and CCN concentrations in red, especially at low supersaturations (as indicated by a lower applied temperature gradient within the CCN counter, in blue). By contrast, the CCN-active fraction during cloud free time periods at WFM was typically >90% at supersaturations above ~0.6% (Zhang et al. 2019), indicating

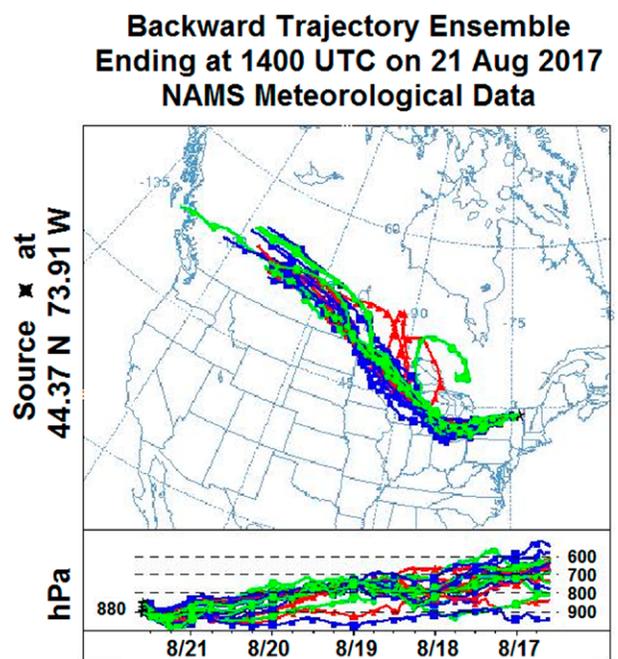a high degree of internal mixing, characteristic of a remote background site. Assuming activated droplets grow by condensation to a diameter >10 μm and are thereby excluded by the PM_{10} aerosol inlet, the in-cloud CCN-active fraction at a given supersaturation indirectly indicates the ambient supersaturation upon which the cloud droplets formed, according to the following logic:

1) Particles that are CCN-active, with a critical supersaturation (S_c) less than the ambient cloud supersaturation (S_{amb}), are excluded by the aerosol inlet.
2) Subsequently, within the CCN counter, only those particles with critical supersaturation less than the imposed instrument supersaturation (S_{instr}) act as CCN.
3) For interstitial particles to be CCN-active under both sets of conditions, that would mean S_{amb} < S_c < S_{instr} (with the implicit assumption that S_c does not change after undergoing a dehydration/rehydration cycle).
4) S_{amb} can then be estimated by systematically varying S_{instr}. If no particles activate within the CCN counter at a given S_{instr}, this indicates that either there were no interstitial particles present (because all aerosol particles were CCN-active at S_{amb}) or that S_{instr} < S_{amb}.
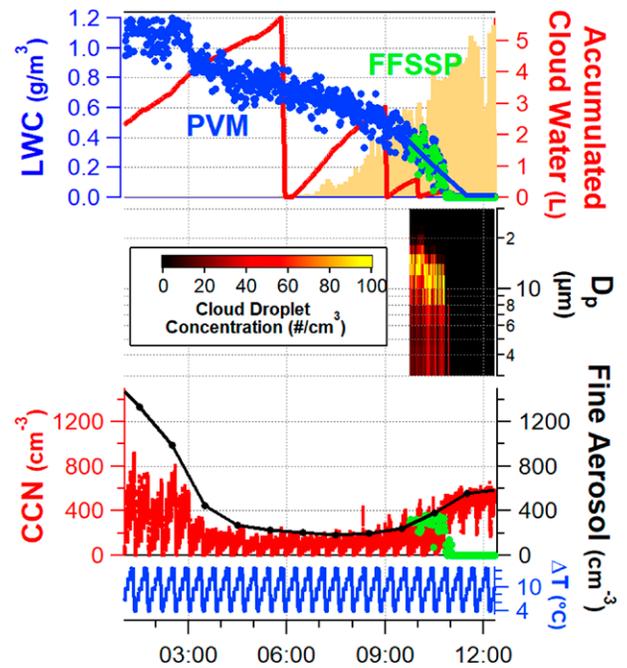

Fig. 8. WFM summit observations from the morning of 13 Aug during the pilot study. Cloud liquid water content (LWC) as measured by the Gerber PVM (blue) and the FFSSP (green) are highlighted. Also shown is solar radiation (yellow) and accumulated volume of cloud water (red), the cloud droplet size distribution as measured by the FFSSP (where D_p represents the droplet diameter), non-size-resolved CCN and fine aerosol concentrations (red and black, respectively), cloud droplet concentrations (green), and the temperature gradient applied to the CCN counter (blue).

Note that even at S_{instr} of 0.78% (the maximum supersaturation applied in our measurements), a measurable concentration of unactivated particles was typically present according to the below-cloud CCN measurements reported by Zhang et al. (2019), suggesting that interstitial particles are generally present, assuming that S_{amb} for the low-altitude orographic clouds at WFM is not significantly >0.78%. The minimum supersaturation at which particles begin to activate within the CCN counter indicates when S_{instr} is slightly above S_{amb}. Using this method, S_{amb} under which the cloud droplets formed is inferred to have ranged from 0.23% to 0.51% on the morning of 13 August. Note that after cloud base had lifted above the summit and clear air was again sampled (at ~1100 local time, LT), ~50% of particles were activated even at the lowest supersaturation applied in the CCN counter (Fig. 8). By inference, these particles were the CCN upon which cloud droplets formed in the recently sampled cloud and were therefore not observed during in-cloud sampling because they were excluded by the PM_{10} aerosol inlet.

As indicated above, cloud droplet size is an important variable for interpreting the in-cloud aerosol measurements, as well as many processes involved in aerosol–cloud interactions. Thus, the FFSSP observations were an important addition to the suite of instruments deployed during CPOC. However, the performance of this FFSSP instrument has not previously been tested at the WFM summit, which frequently experiences strong and variable winds. Average wind speeds throughout the summer months as measured at the WFM summit in 2017 were 7.5 ± 4.3 m s^{-1}, with higher wind speeds frequently observed during in-cloud time periods. To evaluate the FFSSP performance, LWC comparisons were made with Gerber PVM measurements (as highlighted in both Figs. 8 and 9). The first FFSSP observations of the pilot

study, which began at 0945 LT 13 August as cloud base was starting to rise above the WFM summit, yielded LWC based on the measured droplet size distribution that was 5% higher than the PVM LWC (with $R^2 = 0.97$) (Fig. 8). Note that the FFSSP orientation was not yet actively monitored and controlled on this day, but the wind speeds were relatively light (~5 m s^{-1}) and the FFSSP had been manually positioned into the wind at the start of sampling.

The observations on 19–20 August give a clearer indication for the FFSSP performance under different inlet orientations relative to the wind (Fig. 9).

Fig. 9. (a) Droplet size distribution as reported by the FFSSP over two different time intervals, t_1 and t_2, corresponding to the starting position and the ending position of the rotating platform, respectively. (b) Comparison between LWC as reported at 1 min intervals by the Gerber PVM (blue) and LWC calculated from the FFSSP droplet size distribution at 1 s intervals (green). (c) Expanded view of (b) showing the periodicity of the FFSSP LWC at ~5 min intervals. Droplet size distributions (with yellow indicating higher number concentrations and black indicating lower number concentrations) are also shown in (b) and (c). Droplets >~10 μm are undersampled by the FFSSP when oriented at 76° relative to the wind, at wind speeds of ~10 m s^{-1}.

During the time periods shown, the turntable orientation was set with a fixed starting position pointing north, then rotated to point directly into the wind, and subsequently returned to the starting position, over ~5 min intervals. The predominant wind speed and direction was on average 10 m s^{-1} and 285°, respectively, during this time period. When positioned at the starting position, corresponding to a ~76° angle relative to the predominant wind direction, transmission efficiency of droplets through the FFSSP inlet substantially decreased. This effect is most clearly observed in the time series of LWC as calculated from the droplet size distributions, which periodically dipped below 0.1 g m^{-3} at ~5 min intervals corresponding to rotation of the FFSSP platform back to the starting position (Fig. 9c). These sudden dips in LWC are due to loss of droplets >10 μm (Fig. 9a) when positioned at ~76° relative to the predominant winds. Figure 9b highlights two time periods during the rotation of the FFSSP platform, with t_1 representing a 5 s period while held at the starting position and t_2 representing a 10 s period after the platform had been rotated to face the wind. Unfortunately, the precise angle at which droplets are no longer efficiently transmitted through the FFSSP inlet is not known since the transient behavior of the turntable is not precisely known. Only the two extreme resting positions are known with confidence since the speed of the turntable during rotation was not constant. In the future, an independent measure of the turntable orientation will be implemented to prevent ambiguity about this important diagnostic variable, which will be especially important when leaving the FFSSP unattended for extended time periods. Transmission efficiency of the FFSSP inlet is also expected to depend upon droplet size and wind speed, which will require further systematic study.

Below-cloud observations. Observations obtained at the LPT provide a fundamental baseline for aerosol chemical composition at WFM with which to compare the cloud water chemical composition measurements. The CPOC study was the first time a HR-ToF-AMS was deployed to WFM and provided the opportunity to evaluate the organic carbon oxidation state (Canagaratna et al. 2015), from which the organic aerosol mass can be estimated from the routine TOC measurements, as well as the time-varying concentrations of different organic factors, which can help to identify the sources and chemical processing of organic compounds (Zhang et al. 2005). An overview of below-cloud observations obtained at the
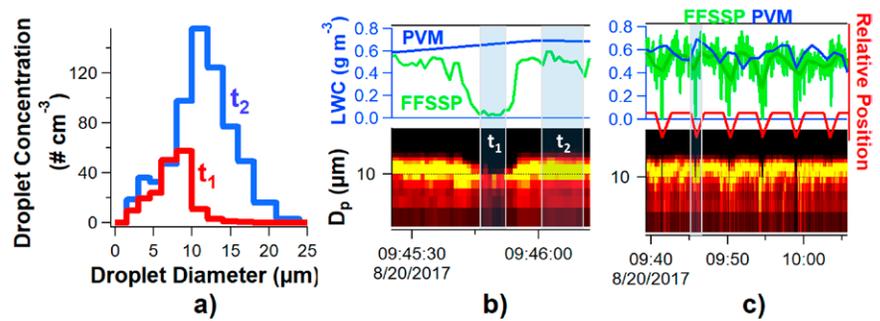
LPT during the CPOC pilot study, as well as a comparison between below-cloud and in-cloud (interstitial) measurements of aerosol composition at the LPT is provided by Zhang et al. (2019). The most striking observation during the pilot study was the dominance of organic aerosol mass, averaging 66%–78% of $PM_{2.5}$ during urban-influenced periods and 83%–93% during biogenic-influenced periods. These observations are in stark contrast to observations in the northeastern United States in past decades when sulfate dominated the submicron aerosol mass loadings (Hand et al. 2012; Blanchard et al. 2019). Even a few years prior to the current study, organic mass measured at WFM was on average only 50% of the total aerosol mass (Schwab et al. 2016b), assuming that OM = 1.8 × OC. The OM:OC ratio for below-cloud aerosols measured during CPOC, calculated using the "Improved Ambient" parameterization (Canagaratna et al. 2015), ranged from 2.14 to 2.40, indicating highly oxidized and aged organic compounds. This suggests that the 0.5 organic mass fraction in 2014 reported by Schwab et al. (2016b) may have been low due to underestimation of the organic oxidation state. Taking the 2.27 average OM:OC ratio obtained during CPOC, the aerosol organic mass fraction in 2014 would have been 0.63 instead of 0.50, 20% lower than the 0.78 average organic mass fraction measured in 2017 during CPOC.

As shown in the "Field sites" section, the ambient cloud supersaturation S_{amb} can be estimated by analyzing non-size-resolved CCN measurements obtained in-cloud (either sampling the interstitial aerosol or the cloud droplet residuals, with the method and limitations for the former described in detail above). The value of S_{amb} can also be estimated by comparing below-cloud and in-cloud aerosol size distributions and size-resolved CCN spectra. Figure 10a shows below-cloud measurements of size-resolved CCN and aerosol particle concentrations, as a function of SMPS scan time after subtracting the time offset between these two parallel measurements (Moore et al. 2010). By comparing the below-cloud observations to in-cloud observations from the WFM summit, the size distribution of CCN particles that activated in-cloud can be inferred (Fig. 10b). To check that the below-cloud aerosol (Fig. 10a) was representative of the aerosol particles upon which the cloud formed, we first compared the below-cloud aerosol size distribution measured at the LPT (Fig. 10b, in black) with the below-cloud
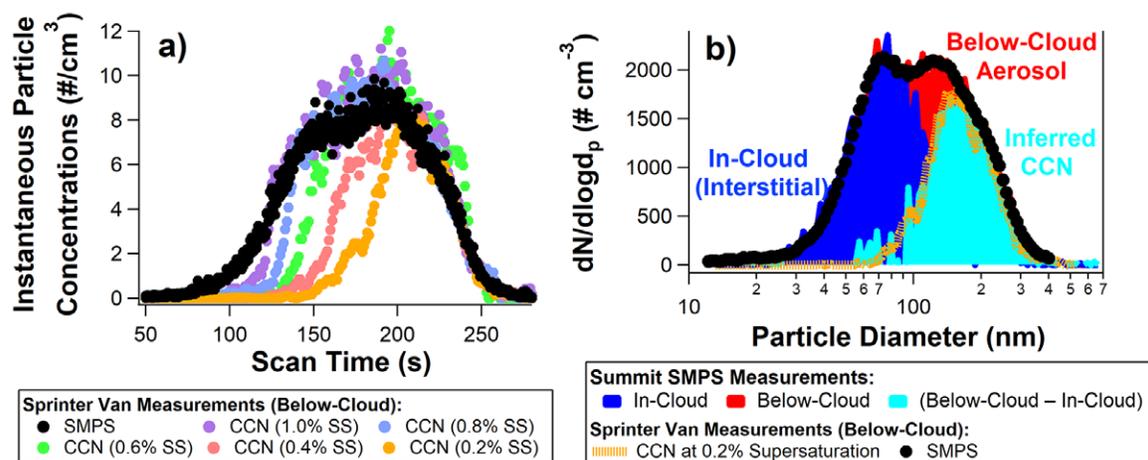

Fig. 10. Aerosol observations obtained on 18 Aug 2017: (a) particle concentrations and CCN concentrations at different instrument supersaturations as a function of SMPS scan time measured below-cloud via the Sprinter van at 1030–1530 LT, and (b) particle size distributions measured at the WFM summit while in-cloud (at 1030–1230 LT) and below-cloud (at 1500–2000 LT) as compared to the Sprinter van measurements reported in (a). "Inferred CCN" concentrations shown in light blue are obtained by subtracting the measured aerosol size distribution in-cloud (representing interstitial aerosol) from the measured aerosol size distribution below-cloud. Supersaturations labeled in this figure are nominal values, corresponding to calibrated values ranging from 0.23% to 0.78% rather than from 0.2% to 1.0%.

aerosol size distribution measured at the summit 1–5 h later, after the cloud had lifted above the summit (Fig. 10b, in red), which showed little disagreement. The inferred CCN distribution (obtained by subtracting the interstitial aerosol size distribution from the below-cloud aerosol size distribution), can then be compared to the CCN distribution measured below-cloud at different supersaturations (Fig. 10b, at S_{instr} = 0.23% in yellow). The good agreement between inferred and measured CCN distributions for this example suggests that S_{amb} ~ 0.23%. The CCN distribution for this example is also consistent with the larger size mode in the aerosol size distribution, often thought to be produced through cloud processing of particles (Hudson et al. 2015).

Note that the size-resolved CCN measurements during CPOC often suffered from low counting statistics due to four primary factors: 1) CCN concentrations at WFM, a remote background site, are not extremely high (generally < 2,000 cm^{-3}, as shown in Fig. 5); 2) size-resolved CCN measurements reduce aerosol concentrations by a factor of ~100 due to the DMA transfer function and the submicron aerosol charging efficiency; 3) wet scavenging removes more CCN-active particles during in-cloud sampling behind the PM$_{10}$ aerosol inlet; and 4) limited sample flow through the SMPS required diluting the monodisperse aerosol sample flow with filtered air to provide sufficient sample flows to the downstream CCN counter and CPC. To obtain reliable CCN distributions and aerosol hygroscopicity values, multiple hour-long supersaturation scans often needed to be averaged together to reduce measurement noise due to these factors. A particle concentrator would help to prevent the need for such long averaging intervals.

Discussion about the CPOC experimental design and additional measurement needs

A specific goal for the CPOC pilot study, as discussed at the 2016 Cloud Water Chemistry Workshop (Lance et al. 2017), was to evaluate meteorological conditions and suitability of the WFM site for assessing cloud processing of organic compounds.

While it is now commonly understood that, under controlled and idealized conditions in the laboratory, aqueous-phase reactions of water soluble organic gases can produce less volatile organic compounds (Carlton et al. 2007; Tan et al. 2009; De Haan et al. 2009; Shapiro et al. 2009; Lim et al. 2010; Sun et al. 2010; Tan et al. 2010; Monge et al. 2012; Lee et al. 2013; Paciga et al. 2014; Yu et al. 2014; George et al. 2015), definitive evidence of aqueous SOA formation in the real world is relatively rare (Dall'Osto et al. 2009; Sullivan et al. 2016; Gilardoni et al. 2016; Bi et al. 2016; Lin et al. 2017; G. Zhang et al. 2017; Kim et al. 2019) due in part to several challenges: Aqueous SOA formation in the ambient environment depends on 1) multiphase interactions (between the gas, aerosol, and cloud phases); 2) the history of an air mass, including the history of relative humidities and sunlight that aerosols have been exposed to while cycling in and out of cloud; 3) the complex chemical mix of gases and particles entrained into clouds, which can also chemically evolve throughout the day or shift with changes in wind direction; and 4) physical processes occurring within clouds, such as wet deposition or particle coagulation, that remove particles or otherwise alter the particle size distribution.

Short-term coordinated field campaigns targeting these type of multiphase interactions have been designed around orographic clouds by stationing measurements at a site upwind and downwind of a hilltop, with in situ cloud measurements stationed in between, to directly compare the "before" and "after" cloud-processing states of the aerosol. Such focused intensive studies have been conducted during several campaigns at high-elevation sites in the United Kingdom and Germany (Wobrock et al. 1994; Bower et al. 1999; Herrmann et al. 2005; Mertes et al. 2005a,b; van Pinxteren et al. 2005; Henning et al. 2014; van Pinxteren et al. 2016; Schneider et al. 2017), which have grown more focused on organic compounds over time. However, the limited meteorological conditions under which "connected flow" is attained

between the upwind, summit, and downwind sites (Heinold et al. 2005; Tilgner et al. 2005, 2014) may limit the applicability of this strategy at other sites.

While we were able to select a suitable upwind site for the CPOC pilot study (the LPT), an appropriate downwind site could not be identified. The WFM lodge is often downwind of the summit and is well equipped to support many additional measurements, but the complex topography, steep terrain, and dense alpine forest upwind of the lodge make it challenging to directly connect observations at the WFM summit and lodge sites due to perturbations introduced by the mountain itself and potential loss of cloud droplets by deposition. Other potential downwind locations on the mountain lack the required power, data, and accessibility due to the site being centered within an undeveloped region of the Adirondack Mountains.

The lack of a suitable downwind measurement site was acknowledged early during planning for the pilot study and an alternative plan was devised. During CPOC, we planned to measure the below-cloud aerosol from an upwind site and compare these observations to aerosols intercepting the summit "between cloud events." This plan is illustrated in Fig. 11a. The idea was that, in a homogeneous field of low-altitude "fair-weather" cumulus intercepting the WFM summit, individual stratocumulus clouds would pass by, and air masses between clouds intercepting the summit would have been recently cloud processed. Under these conditions, we could then investigate differences between measurements of aerosol chemical and physical properties at the two mountain sites to identify any influence of cloud processing.
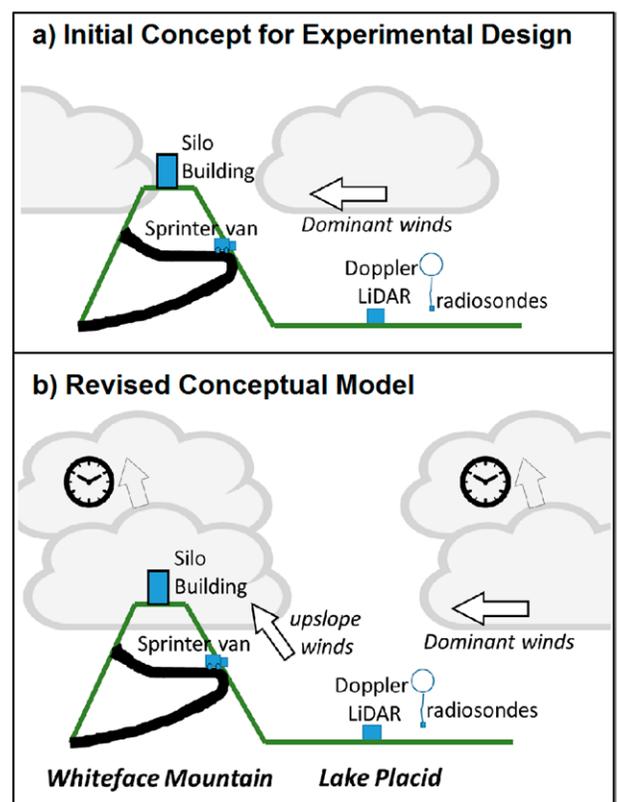

Fig. 11. (a) The initial concept behind the CPOC pilot study experimental design was to compare below-cloud aerosol measurements (from the Sprinter van) with between-cloud aerosol measurements (obtained at the summit). However, orographic uplift precluded time periods between clouds at the summit. (b) The revised conceptual model for fair-weather meteorological conditions at WFM during the summertime, instead, is that cloud base (which tends to lower during the night and rise during the day) dictates whether or not clouds will be intercepting the WFM summit at any given time, even when there are clear-air patches upwind of the summit.

During the pilot study (mid- to late August), cloud behavior did not match the conceptual model from Fig. 11a. Fair-weather cumulus upwind of the summit did exhibit clear patches between clouds (Fig. 12). However, on days when the lifting condensation level (LCL) was below the summit level, there were exceptionally few clear-air patches at the summit until growth of the daytime convective boundary layer caused LCL and cloud base to rise above the summit level. In spite of the 25 km topographic isolation and ~1 km prominence of the WFM summit, the persistent cloudiness at the summit was apparently due to local orographic forcing during ascent, including some combination of mechanical forcing and thermal forcing, as solar heating of the terrain drove thermally direct upslope flows (e.g., Kirshbaum et al. 2018). This orographic forcing also likely increased the cloud supersaturation, cloud depth, and LWC, compared to the surrounding, unperturbed cloud field. Thus, we were unable to directly compare aerosols from recently detrained cloud parcels to below-cloud aerosols, as intended at the outset, because there were no significant between-cloud events sampled at the summit. Instead, only below-cloud and in-cloud conditions were encountered. A revised conceptual framework is illustrated in Fig. 11b.

Clouds that intercepted the summit of WFM during the CPOC pilot study were not entirely orographic, either. Because the daytime boundary layer was generally well mixed (as evidenced by the wind lidar measurements), and the stratocumulus cloud field upwind of WFM ubiquitous (Fig. 12), aerosols measured below-cloud likely experienced multiple cycles through cloud prior to arrival at the LPT. While the ubiquity of fair-weather cumulus may be ideal for promoting aqueous chemical processing due to the abundance of sunlight and high probability of repeated aerosol–cloud cycling (Tsui et al. 2019), this further challenges our strategy for identifying before and after cloud processing states of the aerosol.

Several desirable characteristics of the WFM site, such as the frequency with which the summit intercepts clouds, the remote and isolated peak and the location downwind of different emissions sources from the United States and Canada, motivate us to consider other strategies to compensate for lack of a suitable downwind site. Also note that, in comparison to the previously cited high elevation studies of cloud processing, CPOC observations showed very high organic mass fractions. For example, during the Hill Cap Cloud Thuringia 2010 (HCCT-2010) field campaign at a forested hilltop in central Germany, organics comprised only 20%–40% of the cloud water solute mass (van Pinxteren et al. 2016), while observations during CPOC showed that organics comprised 78% of the aerosol mass on average, growing to 83%–93% during biogenic influenced periods (Zhang et al. 2019). Thus, in many ways WFM is ideally suited to the study of chemical processing of organics within clouds.

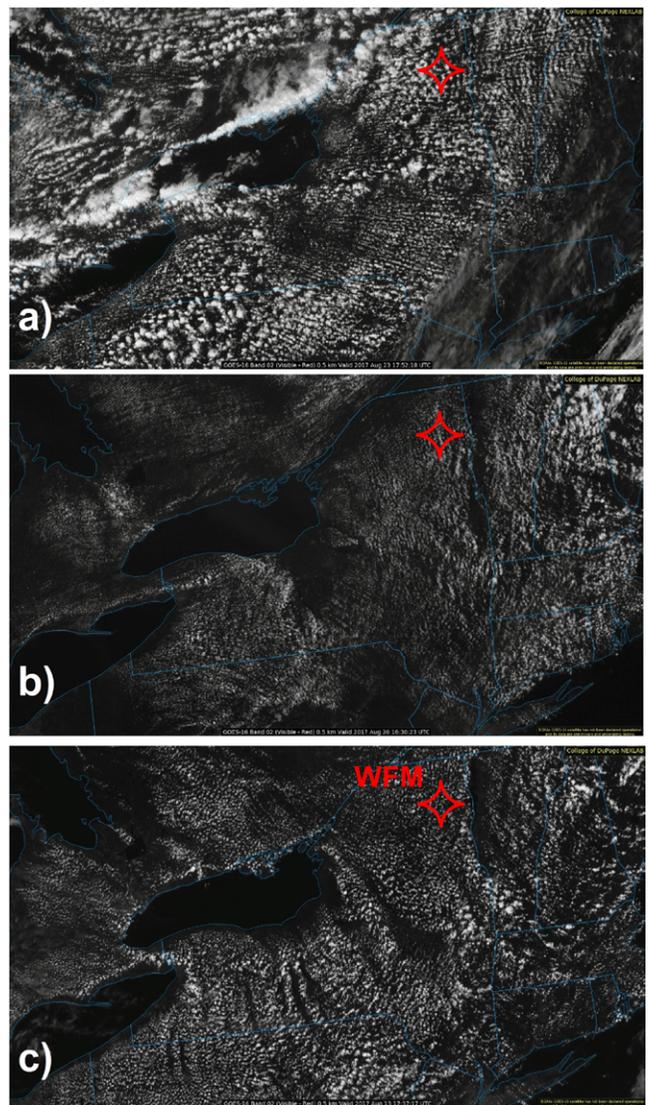Previous research at WFM was successful in identifying source–receptor relationships for

Fig. 12. GOES visible images centered on New York State during the CPOC pilot study, at (a) 1300 LT 23 Aug, (b) 1130 LT 20 Aug, and (c) 0030 LT 13 Aug. In all cases, cloud base was just rising above the WFM summit when the image was captured. The widespread cumulostratus over New York State on most days throughout the summertime suggest that aerosols were cloud-processed prior to arriving at WFM.

heterogeneously produced compounds using tracer compounds measured at multiple sites. This method evaluated changes in the sulfate to tracer concentration during transport from one site to another and relied upon these tracer compounds being directly tied to SO_2 emissions from coal combustion while not being produced by other mechanisms in the atmosphere (Husain and Dutkiewicz 1992; Burkhard et al. 1995; Rattigan et al. 2001). A similar path forward might be pursued for organic compounds. However, since the chemical evolution of organics in the atmosphere is so complex, with precursors from many distinct and often diffuse sources (both natural and anthropogenic), this type of tracer method could very well be intractable for organics.

Various ways for assessing the before and after cloud processing states of ambient aerosol have been pursued by researchers at other fixed sites. As discussed previously, one way to accomplish this goal is to make measurements at upwind and downwind sites under conditions

where changes in the aerosol can be clearly attributed to cloud processing between the two sites. However, accomplishing this task may not be feasible at all sites or under many meteorological situations. An alternative strategy is to compare below-cloud aerosol composition with cloud droplet residuals or re-aerosolized (and dried) cloud water to infer changes due to cloud processing (Lee et al. 2012). Re-aerosolized cloud water and cloud droplet residuals can be clearly identified as "cloud processed," since they, by necessity, must be obtained in-cloud. The degree of cloud processing will depend on the transit time from cloud base to the in-cloud sampling site (which, for a 234 m elevation gain between the LPT and the WFM summit, corresponds to ~2 min, assuming an updraft velocity of 2 m s⁻¹ and cloud base positioned right at the LPT). Collocated measurements of cloud droplet residuals and cloud water composition can be obtained by operating a ground-based Counterflow Virtual Impactor (gCVI) (Shingler et al. 2012; Lin et al. 2017; G. Zhang et al. 2017) alongside the cloud water collector (Wobrock et al. 1994; Lee et al. 2012; van Pinxteren et al. 2016) to yield crucial information about partitioning of organic and inorganic compounds between the gas, aerosol, and cloud phases (Hennigan et al. 2009). By adding below-cloud aerosol measurements to the cloud water and cloud droplet residual measurements, both the before and after cloud processing states can be assessed with only two measurement sites. Further chemical processing of the aqueous phase would naturally occur at progressively higher altitudes in the cloud, which can be investigated by exposing the collected cloud water to oxidizing gases and/or radiation under controlled conditions on- or off-site (Lee et al. 2012), taking care to preserve any labile chemical species if storage for any length of time is required.

At a remote site like WFM with an isolated peak typically within a well-mixed boundary layer (during the summertime), it is relatively easy to find an upwind site that is representative of aerosols lofted into cloud. The LPT may be the best choice since it is the nearest drivable upwind location (both horizontally and vertically) that is frequently below-cloud during the daytime. But, for long-term measurements, the LPT would be impractical since there is no permanent structure there. Other sites, like the Gabriels Mesonet station or Paul Smith's college <30 km west of WFM may be sufficient as an upwind site, if measurements can be obtained at sufficient heights to be within the well-mixed boundary layer.

A further consideration for bulk cloud water measurements is the lack of information on the aerosol mixing state. Droplets formed on coarse mode aerosol (such as pollen, sea spray, or mineral dust) exist in separate microenvironments from other cloud droplets in the atmosphere. Mineral dust and cloud droplets can coagulate and chemically react with one another in the atmosphere, but coagulation can only decrease (not increase) the number of mineral dust containing droplets. Based on the number concentrations of cloud condensation nuclei and coarse mode aerosol, by logical inference, most droplets cannot contain mineral dust or other coarse mode aerosol particles. Thus, the measured Na^+, Mg^{2+}, Ca^{2+}, and K^+ ions associated with coarse mode aerosol exist within a small subset of the droplets, and we can assume that the vast majority of droplets (produced through secondary formation pathways) do not contain these alkaline metal ions at all. However, we know that these nonvolatile cations can contribute significantly to the soluble mass, ion balance, and pH of bulk cloud water (Dukett et al. 2011) and aerosol (Guo et al. 2018). This implies that the bulk cloud water composition can be distinct from the natural atmospheric state of cloud droplets produced from either aerosol mode (Pye et al. 2020). To really understand chemical processing of organics in clouds, the impact of mixing state needs to be assessed. When sampling cloud droplet residual particles, an impactor can be used to remove the supermicron particles prior to chemical analysis. By sampling cloud droplet residuals with and without the impactor, and comparing to the bulk cloud water composition, ambiguities in the cloud water composition associated with aerosol mixing state can be assessed. An added advantage of using a gCVI is that it concentrates the cloud droplet residuals (relative to their ambient concentrations), thereby improving the

Table 2. List of recommended measurements for a two-site campaign at WFM targeting the impact of cloud processing on aerosol chemical composition. Meteorological conditions such as humidity, temperature, wind direction and speed, solar radiation, and the presence of clouds/precipitation should be obtained at both sites. PILS-IC/TOC refers to particle-into-liquid sampling followed by ion chromatography and TOC analysis (Sullivan et al. 2004), providing directly comparable information about the aerosol and cloud composition, which can also be compared to the routine long-term measurements. AMS refers to aerosol mass spectrometry, which should also be conducted at both sites to better characterize the inorganic and organic aerosol mass. Measurements using proton transfer reaction mass spectrometry (PTRMS), chemical ionization mass spectrometry (CIMS), and/or gas chromatography (GC) at the summit are needed to characterize volatile organic compounds (VOCs). Due to the continuum of volatility for organic compounds, it would be beneficial to conduct chemical speciation of organic aerosols and gases in tandem using the FIGAERO inlet (Lopez-Hilfiker et al. 2014) and/or TAG-AMS (Williams et al. 2014).

Sampling location	Key measurements	Recommended instruments/analyses/sampling
WFM summit	Cloud water chemical composition	TOC, IC, pH, H_2O_2, organic speciation, drop-size-resolved
	Chemical composition of droplet residuals	AMS, PILS-IC/TOC, gCVI, impactor
	Volatile organic compounds	PTRMS, CIMS, GC
	Oxidants/inorganic trace gases	NO, NO_y, O_3, H_2O_2, HNO_3, SO_2, NH_3
Upwind site	Below-cloud aerosol composition	AMS, PILS-IC/TOC
	Volatile organic compounds	PTRMS, CIMS, GC
	Oxidants/inorganic trace gases	NO, NO_y, O_3, H_2O_2, HNO_3, SO_2, NH_3

signal to noise ratio and/or measurement time resolution. Droplet size-resolved cloud water sampling would also provide information on the mixing state, in addition to differences in dilution between smaller and larger droplets (Moore et al. 2004a,b). Table 2 gives a summary of additional recommended measurements and instruments for a future WFM cloud chemistry study, after reflecting upon experience gained during the pilot study.

Summary

The CPOC pilot study at Whiteface Mountain (WFM) in August 2017 was a first step toward experimentally evaluating the chemical processing of organics within clouds, using existing ASRC infrastructure and instruments. The ASRC Sprinter van was deployed to the site, and was a measurement platform for below-cloud aerosol measurements during select time periods. Clouds and organic aerosols were both found to be ubiquitous during the pilot study, underscoring the potential importance of their interactions and the utility of the site for measuring these interactions. In this paper, intercomparisons between measurements of interstitial aerosols, CCN, and cloud droplets are shown. We also highlight observations consistent with long-range transport of biomass burning smoke, which appears to be scavenged efficiently by clouds.

Specialized in situ instruments were deployed to the WFM site for the first time during CPOC, including a HR-ToF-AMS, FFSSP, and CCNc, which complemented the long-term measurements routinely obtained at WFM and provided valuable additional information about the aerosol chemical composition, cloud microphysics, and cloud–aerosol interactions. Future coordinated measurements at WFM, and potentially other mountain sites, can take advantage of lessons learned during our pilot study, as described in this paper. In particular, we found that stratocumulus clouds intercepting WFM were neither fully convective nor fully orographic, preventing us from measuring between-cloud aerosols at the summit to compare with the below-cloud aerosol measurements and preventing us from confidently measuring cloud-processed aerosols at a downwind site. We conclude that sampling of cloud droplet residuals would be a key addition for future field campaigns at WFM targeting aerosol–cloud interactions, as a means for more clearly identifying and targeting cloud-processed aerosol. In

conjunction with the cloud water composition, these measurements would also provide valuable information about gas–aerosol and gas–cloud water phase partitioning. Measurements of volatile organic compounds and other soluble gases would further fill the gap between the cloud water, droplet residual, and below-cloud aerosol measurements.

An overview of below-cloud aerosol observations during the CPOC pilot study has been published by Zhang et al. (2019), and future focused papers discussing other aspects of the pilot study in more detail are expected, including 1) intercomparison between various offline measurements of cloud water chemical composition and properties, 2) cloud microphysics observations in the context of WFM cloud climatology, and 3) retrieval of aerosol optical properties using Doppler lidar and sun photometer observations.

While air quality has improved over the past several decades due to targeted emissions reductions, our understanding of multiphase chemical processes, especially in relation to organics, remains incomplete. Human emissions also continue to evolve, even as ecosystems continue to respond to previously emitted pollutants. Significant advancements in measurement capabilities with respect to organic compounds in both the gas and particle phase have been made over the past several decade. The research observatory at Whiteface Mountain provides a powerful platform for using new tools to tackle chemically complex processes occurring within clouds, both in future coordinated campaigns and with routine long-term measurements.

Data availability statement. CPOC pilot study data, back trajectories and aerosol forecast model results are archived at http://atmoschem.asrc.cestm.albany.edu/~cpoc/.

References

Aleksic, N., K. Roy, G. Sistla, J. Dukett, N. Houck, and P. Casson, 2009: Analysis of cloud and precipitation chemistry at Whiteface Mountain, NY. *Atmos. Environ.*, **43**, 2709–2716, https://doi.org/10.1016/j.atmosenv.2009.02.053.

Anderson, J., R. Baumgardner, V. Mohnen, and J. Bowser, 1999: Cloud chemistry in the eastern United States, as sampled from three high-elevation sites along the Appalachian Mountains. *Atmos. Environ.*, **33**, 5105–5114, https://doi.org/10.1016/S1352-2310(99)00193-4.

Baumgardner, R. E., Jr., S. S. Isil, T. F. Lavery, C. M. Rogers, and V. A. Mohnen, 2003: Estimates of cloud water deposition at mountain acid deposition program sites in the Appalachian Mountains. *J. Air Waste Manage. Assoc.*, **53**, 291–308, https://doi.org/10.1080/10473289.2003.10466153.

Bi, X., and Coauthors, 2016: In situ detection of the chemistry of individual fog droplet residues in the Pearl River Delta region, China. *J. Geophys. Res. Atmos.*, **121**, 9105–9116, https://doi.org/10.1002/2016JD024886.

Blanchard, C., S. Shaw, E. Edgerton, and J. Schwab, 2019: Emission influences on air pollutant concentrations in New York state: II. $PM_{2.5}$ organic and elemental carbon constituents. *Atmos. Environ.*, **3**, 100039, https://doi.org/10.1016/J.AEAOA.2019.100039.

Bower, K., and Coauthors, 1999: The Great Dun fell experiment 1995: An overview. *Atmos. Res.*, **50**, 151–184, https://doi.org/10.1016/S0169-8095(98)00103-3.

Brandt, R. E., and Coauthors, 2016: Atmospheric chemistry measurements at Whiteface Mountain, NY: Ozone and reactive trace gases. *Aerosol Air Qual. Res.*, **16**, 873–884, https://doi.org/10.4209/aaqr.2015.05.0376.

Burkhard, E., B. Ghauri, V. Dutkiewicz, and L. Husain, 1995: A multielement tracer technique for the determination of SO_2 oxidation in clouds. *J. Geophys. Res.*, **100**, 26051–26059, https://doi.org/10.1029/95JD01939.

Canagaratna, M., and Coauthors, 2015: Elemental ratio measurements of organic compounds using aerosol mass spectrometry: Characterization, improved

calibration, and implications. *Atmos. Chem. Phys.*, **15**, 253–272, https://doi.org/10.5194/acp-15-253-2015.

Carlton, A., B. Turpin, K. Altieri, S. Seitzinger, A. Reff, H.-J. Lim, and B. Ervens, 2007: Atmospheric oxalic acid and SOA production from glyoxal: Results of aqueous photooxidation experiments. *Atmos. Environ.*, **41**, 7588–7602, https://doi.org/10.1016/j.atmosenv.2007.05.035.

——, C. Wiedinmyer, and J. Kroll, 2009: A review of secondary organic aerosol SOA formation from isoprene. *Atmos. Chem. Phys.*, **9**, 4987–5005, https://doi.org/10.5194/acp-9-4987-2009.

Chen, Z., O. Torres, P. Bhartia, D. Flittner, G. Taha, and K. Leavor, 2018: Multi-sensor view of the stratospheric carbonaceous aerosol layer from 2017 Boreal fires in Canada. *2018 AGU Fall Meeting*, Washington, DC, Amer. Geophys. Union, Abstract A21J-2829.

Chowdhury, P., Q. He, T. Male, W. Brune, Y. Rudich, and M. Pardo, 2018: Exposure of lung epithelial cells to photochemically aged secondary organic aerosol shows increased toxic effects. *Environ. Sci. Technol. Lett.*, **5**, 424–430, https://doi.org/10.1021/acs.estlett.8b00256.

Civerolo, K., O. Rattigan, H. Felton, and J. Schwab, 2017: Changes in gas-phase air pollutants across New York State, USA. *Aerosol Air Qual. Res.*, **17**, 147–166, https://doi.org/10.4209/aaqr.2016.04.0141.

Cook, R., and Coauthors, 2017: Biogenic, urban, and wildfire influences on the molecular composition of dissolved organic compounds in cloud water. *Atmos. Chem. Phys.*, **17**, 15 167–15 180, https://doi.org/10.5194/acp-17-15167-2017.

Dall'Osto, M., R. Harrison, H. Coe, and P. Williams, 2009: Real-time secondary aerosol formation during a fog event in London. *Atmos. Chem. Phys.*, **9**, 2459–2469, https://doi.org/10.5194/acp-9-2459-2009.

Das, S., P. Colarco, L. Oman, G. Tweedy, O. Taha, O. Torres, and D. Peterson, 2018: The three-dimensional evolution of smoke aerosols emitted during the 2017 pyrocumulonimbus events over British Columbia. *2018 AGU Fall Meeting*, Washington, DC, Amer. Geophys. Union, Abstract A23E-08.

De Haan, D., A. Corrigan, M. Tolbert, J. Jimenez, S. Wood, and J. Turley, 2009: Secondary organic aerosol formation by self-reactions of methylglyoxal and glyoxal in evaporating droplets. *Environ. Sci. Technol.*, **43**, 8184–8190, https://doi.org/10.1021/es902152t.

Ditto, J., and Coauthors, 2018: An omnipresent diversity and variability in the chemical composition of atmospheric functionalized organic aerosol. *Nat. Comm. Chem.*, **1**, 75, https://doi.org/10.1038/S42004-018-0074-3.

Draxler, R., and G. Hess, 1998: An overview of the HYSPLIT 4 modeling system of trajectories, dispersion, and deposition. *Aust. Meteor. Mag.*, **47**, 295–308.

Drewnick, F., and Coauthors, 2005: A new Time-of-Flight Aerosol Mass Spectrometer (TOF-AMS)—Instrument description and first field deployment. *Aerosol Sci. Technol.*, **39**, 637–658, https://doi.org/10.1080/02786820500182040.

Dukett, J., N. Aleksic, N. Houck, P. Snyder, P. Casson, and M. Cantwell, 2011: Progress toward clean cloud water at Whiteface Mountain New York. *Atmos. Environ.*, **45**, 6669–6673, https://doi.org/10.1016/j.atmosenv.2011.08.070.

Ehn, M., and Coauthors, 2014: A large source of low-volatility secondary organic aerosol. *Nat. Lett.*, **506**, 476–479, https://doi.org/10.1038/nature13032.

Ervens, B., 2015: Modeling the processing of aerosol and trace gases in clouds and fogs. *Atmos. Chem. Rev.*, **12**, 10 353–10 365, https://doi.org/10.5194/acp-12-10353-2012.

——, B. Turpin, and R. Weber, 2011: Secondary organic aerosol formation in cloud droplets and aqueous particles (aqSOA): A review of laboratory, field and model studies. *Atmos. Chem. Phys.*, 11 069–11 102, https://doi.org/10.5194/acp-11-11069-2011.

——, Y. Wang, W. Leaitch, A. Macdonald, K. Valsaraj, and P. Herckes, 2013: Dissolved organic carbon (DOC) and select aldehydes in cloud and fog water: The role of aqueous phase in impacting trace gas budgets. *Atmos. Chem. Phys.*, **13**, 5117–5135, https://doi.org/10.5194/acp-13-5117-2013.

Falconer, R., and P. Falconer, 1980: Determination of cloud water acidity at a mountain observatory in the Adirondack Mountains of New York State. *J. Geophys. Res.*, **85**, 7465–7470, https://doi.org/10.1029/JC085iC12p07465.

Farmer, D., C. Cappa, and S. Kreidenweis, 2015: Atmospheric processes and their controlling influence on cloud condensation nuclei activity. *Chem. Rev.*, **115**, 4199–4217, https://doi.org/10.1021/cr5006292.

Gelencsér, A., and Z. Varga, 2005: Evaluation of the atmospheric significance of multiphase reactions in atmospheric secondary organic aerosol formation. *Atmos. Chem. Phys.*, **5**, 2823–2831, https://doi.org/10.5194/acp-5-2823-2005.

George, C., M. Ammann, B. D'Anna, D. Donaldson, and S. Nizkorodov, 2015: Heterogeneous photochemistry in the atmosphere. *Chem. Rev.*, **115**, 4218–4258, https://doi.org/10.1021/cr500648z.

Gerber, H., 1991: Direct measurement of suspended particulate volume concentration and far-infrared extinction coefficient with a laser-diffraction instrument. *Appl. Opt.*, **30**, 4824–4831, https://doi.org/10.1364/AO.30.004824.

Gilardoni, S., and Coauthors, 2016: Direct observation of aqueous secondary organic aerosol from biomass-burning emissions. *Proc. Natl. Acad. Sci. USA*, **113**, 102013–102018, https://doi.org/10.1073/pnas.1602212113.

Guo, H., A. Nenes, and R. Weber, 2018: The underappreciated role of nonvolatile cations in aerosol ammonium-sulfate molar ratios. *Atmos. Chem. Phys.*, **18**, 172307–172323, https://doi.org/10.5194/acp-18-17307-2018.

Hallquist, M., and Coauthors, 2009: The formation, properties and impact of secondary organic aerosol: Current and emerging issues. *Atmos. Chem. Phys.*, **9**, 5155–5236, https://doi.org/10.5194/acp-9-5155-2009.

Hand, J., B. Schichtel, W. Malm, and M. Pitchford, 2012: Particulate sulfate ion concentration and SO_2 emission trends in the United States from the early 1990s through 2010. *Atmos. Chem. Phys.*, **12**, 10 353–10 365, https://doi.org/10.5194/acp-12-10353-2012.

Heald, C., D. Jacob, R. Park, L. Russell, B. Huebert, J. Seinfeld, H. Liao, and R. Weber, 2005: A large organic aerosol source in the free troposphere missing from current models. *Geophys. Res. Lett.*, **32**, L18809, https://doi.org/10.1029/2005GL023831.

Heinold, B., A. Tilgner, W. Jaeschke, W. Haunold, O. Knoth, R. Wolke, and H. Herrmann, 2005: Meteorological characterization of the FEBUKO hill cap cloud experiment, Part II: Tracer experiments and flow characterisation with nested non-hydrostatic atmospheric models. *Atmos. Environ.*, **39**, 4195–4207, https://doi.org/10.1016/j.atmosenv.2005.02.036.

Hennigan, C., M. Bergin, A. Russell, A. Nenes, and R. Weber, 2009: Gas/particle partitioning of water-soluble organic aerosol in Atlanta. *Atmos. Chem. Phys.*, **9**, 3613–3628, https://doi.org/10.5194/acp-9-3613-2009.

Henning, S., and Coauthors, 2014: Influence of cloud processing on CCN activation behaviour in the Thuringian forest, Germany during HCCT-2010. *Atmos. Chem. Phys.*, **14**, 7859–7868, https://doi.org/10.5194/acp-14-7859-2014.

Herckes, P., K. Valsaraj, and J. Collett Jr., 2013: A review of observations of organic matter in fogs and clouds: Origin, processing and fate. *Atmos. Res.*, **132–133**, 434–449, https://doi.org/10.1016/j.atmosres.2013.06.005.

Herrmann, H., and Coauthors, 2005: FEBUKO and MODMEP: Field measurements and modelling of aerosol and cloud multiphase processes. *Atmos. Environ.*, **39**, 4169–4183, https://doi.org/10.1016/j.atmosenv.2005.02.004.

——, T. Schaefer, A. Tolgner, S. Styler, C. Weller, M. Teich, and T. Otto, 2015: Tropospheric aqueous-phase chemistry: Kinetics, mechanisms, and its coupling to a changing gas phase. *Chem. Rev.*, **115**, 4259–4334, https://doi.org/10.1021/cr500447k.

Huang, D., Q. Zhang, H. Cheung, L. Yu, S. Zhou, C. Anastasio, J. Smith, and C. Chan, 2018: Formation and evolution of aqSOA from aqueous-phase reactions of phenolic carbonyls: Comparison between ammonium sulfate and ammonium nitrate solutions. *Environ. Sci. Technol.*, **52**, 9215–9224, https://doi.org/10.1021/acs.est.8b03441.

Hudson, J., S. Noble, and S. Tabor, 2015: Cloud supersaturations from CCN spectra Hoppel minima. *J. Geophys. Res. Atmos.*, **120**, 3436–3452, https://doi.org/10.1002/2014JD022669.

Hunter, J., and Coauthors, 2017: Comprehensive characterization of atmospheric organic carbon at a forested site. *Nat. Geo.*, **10**, 748–753, https://doi.org/10.1038/ngeo3018.

Husain, L., 1989: A technique for determining in-cloud formation of SO4. *Geophys. Res. Lett.*, **16**, 57–60, https://doi.org/10.1029/GL016i001p00057.

——, and V. Dutkiewicz, 1990: A long-term (1975–1988) study of atmospheric SO_4^{2-}: Regional contributions and concentration trends. *Atmos. Environ.*, **24**, 1175–1187, https://doi.org/10.1016/0960-1686(90)90082-X.

——, and ——, 1992: Elemental tracers for the study of homogeneous gas phase oxidation of SO_2 in the atmosphere. *J. Geophys. Res.*, **97**, 14 635–14 643, https://doi.org/10.1029/92JD01479.

Isaacman-VanWertz, G., and Coauthors, 2018: Chemical evolution of atmospheric organic carbon over multiple generations of oxidation. *Nat. Chem.*, **10**, 462–468, https://doi.org/10.1038/s41557-018-0002-2.

Jimenez, J., and Coauthors, 2009: Evolution of organic aerosols in the atmosphere. *Science*, **326**, 1525–1529, https://doi.org/10.1126/science.1180353.

Kanakidou, M., and Coauthors, 2005: Organic aerosol and global climate modelling: A review. *Atmos. Chem. Phys.*, **5**, 1053–1123, https://doi.org/10.5194/acp-5-1053-2005.

Kim, H., and Coauthors, 2019: Chemical processing of water-soluble species and formation of secondary organic aerosol in fogs. *Atmos. Environ.*, **200**, 158–166, https://doi.org/10.1016/j.atmosenv.2018.11.062.

Kirshbaum, D., B. Adler, N. Kalthoff, C. Barthlott, and S. Serafin, 2018: Moist orographic convection: Physical mechanisms and links to surface-exchange processes. *Atmosphere*, **9**, 80, https://doi.org/10.3390/ATMOS9030080.

Laing, J., and D. Jaffe, 2019: Wildfires are causing extreme PM concentrations in the western United States. *EM Magazine*, June issue, Air and Waste Management Association, 6 pp., http://pubs.awma.org/flip/EM-June-2019/emjune19.pdf.

Lance, S., J. Medina, J. Smith, and A. Nenes, 2006: Mapping the operation of the DMT continuous flow CCN counter. *Aerosol Sci. Technol.*, **40**, 242–254, https://doi.org/10.1080/02786820500543290.

——, C. Brock, D. Rogers, and J. Gordon, 2010: Water droplet calibration of the Cloud Droplet Probe (CDP) and in-fight performance in liquid, ice and mixed-phase clouds during ARCPAC. *Atmos. Meas. Tech.*, **3**, 1683–1706, https://doi.org/10.5194/amt-3-1683-2010.

——, M. Barth, and A. Carlton, 2017: Multiphase chemistry: Experimental design for coordinated measurement and modeling studies of cloud processing at a mountaintop. *Bull. Amer. Meteor. Soc.*, **98**, ES163–ES167, https://doi.org/10.1175/BAMS-D-17-0015.1.

Lee, A., K. Hayden, P. Herckes, W. Leaitch, J. Liggio, A. Macdonald, and J. Abbatt, 2012: Characterization of aerosols and cloud water at a mountain site during WACS 2010: Secondary organic aerosol formation through oxidative cloud processing. *Atmos. Chem. Phys.*, **12**, 7103–7116, https://doi.org/10.5194/acp-12-7103-2012.

——, R. Zhao, R. Li, J. Liggio, S. Li, and J. Abbatt, 2013: Formation of light absorbing organo-nitrogen species from evaporation of droplets containing glyoxal and ammonium sulfate. *Environ. Sci. Technol.*, **47**, 12 819–12 826, https://doi.org/10.1021/es402687w.

Lee, B., and Coauthors, 2018: Semi-volatile and highly oxygenated gaseous and particulate organic compounds observed above a boreal forest canopy. *Atmos. Chem. Phys.*, **18**, 11 547–11 562, https://doi.org/10.5194/acp-18-11547-2018.

Lim, Y., Y. Tan, M. Perri, S. Seitzinger, and B. Turpin, 2010: Aqueous chemistry and its role in secondary organic aerosol (SOA) formation. *Atmos. Chem. Phys.*, **10**, 10 521–10 539, https://doi.org/10.5194/acp-10-10521-2010.

Lin, M., L. Horowitz, R. Payton, A. Fiore, and G. Tonnesen, 2017: US surface ozone trends and extremes from 1980 to 2014: Quantifying the roles of rising Asian emissions, domestic controls, wildfires, and climate. *Atmos. Chem. Phys.*, **18**, 2943–2970, https://doi.org/10.5194/acp-17-2943-2017.

Lopez-Hilfiker, F., and Coauthors, 2014: A novel method for online analysis of gas and particle composition: Description and evaluation of a Filter Inlet for Gases and AEROsols (FIGAERO). *Atmos. Meas. Tech.*, **7**, 983–1001, https://doi.org/10.5194/amt-7-983-2014.

Lutsch, E., and Coauthors, 2019: Unprecedented atmospheric ammonia concentrations detected in the high Arctic from the 2017 Canadian wildfires. *J. Geophys. Res. Atmos.*, **124**, 8178–8202, https://doi.org/10.1029/2019JD030419.

McNeill, V., 2015: Aqueous organic chemistry in the atmosphere: Sources and chemical processing of organic aerosols. *Environ. Sci. Technol.*, **49**, 1237–1244, https://doi.org/10.1021/es5043707.

Mekis, E., N. Donaldson, J. Reid, A. Zucconi, J. Hoover, Q. Li, R. Nitu, and S. Melo, 2018: An overview of surface-based precipitation observations at environment and climate change Canada. *Atmos. Ocean*, **56**, 71–95, https://doi.org/10.1080/07055900.2018.1433627.

Mertes, S., D. Galgon, K. Schwirn, A. Nowak, K. Lehmann, A. Massling, A. Wiedensohler, and W. Wieprecht, 2005a: Evolution of particle concentration and size distribution observed upwind, inside and downwind hill cap clouds at connected flow conditions during FEBUKO. *Atmos. Environ.*, **39**, 4233–4245, https://doi.org/10.1016/j.atmosenv.2005.02.009.

——, K. Lehmann, A. Nowak, A. Massling, and A. Wiedensohler, 2005b: Link between aerosol hygroscopic growth and droplet activation observed for hill-capped clouds at connected flow conditions during FEBUKO. *Atmos. Environ.*, **39**, 4247–4256, https://doi.org/10.1016/j.atmosenv.2005.02.010.

Möhnen, V., and J. Kadlecek, 1989: Cloud chemistry research at Whiteface Mountain. *Tellus*, **41B**, 79–91, https://doi.org/10.3402/tellusb.v41i1.15052.

——, and R. Vong, 1993: A climatology of cloud chemistry for the eastern United States derived from the Mountain Cloud Chemistry Project. *Environ. Rev.*, **1**, 38–54, https://doi.org/10.1139/a93-005.

Monge, M., and Coauthors, 2012: Alternative pathway for atmospheric particle growth. *Proc. Natl. Acad. Sci. USA*, **109**, 6840–6844, https://doi.org/10.1073/pnas.1120593109.

Moore, K., D. Sherman, J. E. Reilly, and J. Collett Jr., 2004a: Drop size-dependent chemical composition in clouds and fogs. Part I. Observations. *Atmos. Environ.*, **38**, 1389–1402, https://doi.org/10.1016/j.atmosenv.2003.12.013.

——, ——, ——, M. Hannigan, T. Lee, and J. Collett Jr., 2004b: Drop size-dependent chemical composition in clouds and fogs. Part II. Relevance to interpreting the aerosol/trace gas/fog system. *Atmos. Environ.*, **38**, 1403–1415, https://doi.org/10.1016/j.atmosenv.2003.12.014.

Moore, R., A. Nenes, and J. Medina, 2010: Scanning mobility CCN analysis: A method for fast measurements of size-resolved CCN distributions and activation kinetics. *Aerosol Sci. Technol.*, **44**, 861–871, https://doi.org/10.1080/02786826.2010.498715.

NAS, 2016: *The Future of Atmospheric Chemistry Research: Remembering Yesterday, Understanding Today, Anticipating Tomorrow.* The National Academies Press, 207 pp., https://doi.org/10.17226/23573.

Paciga, A., I. Riipinen, and S. Pandis, 2014: Effect of ammonia on the volatility of organic diacids. *Environ. Sci. Technol.*, **48**, 13 769–13 775, https://doi.org/10.1021/ES5037805.

Petters, M., and S. Kreidenweis, 2007: A single parameter representation of hygroscopic growth and cloud condensation nucleus activity. *Atmos. Chem. Phys.*, **7**, 1961–1971, https://doi.org/10.5194/acp-7-1961-2007.

Pye, H., and Coauthors, 2020: The acidity of atmospheric particles and clouds. *Atmos. Chem. Phys.*, **20**, 4809–4888, https://doi.org/10.5194/acp-20-4809-2020.

Rattigan, O., V. Dutkiewicz, M. Das, C. Judd, and L. Husain, 2001: Oxidation of SO_2 in clouds at Whiteface Mountain. *Water Air Soil Pollut. Focus*, **1**, 391–400, https://doi.org/10.1023/A:1013168903087.

——, K. Civerolo, H. Felton, J. Schwab, and K. Demerjian, 2016: Long term trends in New York: PM2.5 mass and particle components. *Aerosol Air Qual. Res.*, **16**, 1191–1205, https://doi.org/10.4209/AAQR.2015.05.0319.

——, ——, and ——, 2017: Trends in wet precipitation, particulate, and gas-phase species in New York State. *Atmos. Pollut. Res.*, **8**, 1090–1102, https://doi.org/10.1016/j.apr.2017.04.007.

Rich, D., and Coauthors, 2019: Triggering of cardiovascular hospital admissions by source specific fine particle concentrations in urban centers of New York State. *Environ. Int.*, **126**, 387–394, https://doi.org/10.1016/j.envint.2019.02.018.

Ridley, D., C. Heald, K. Ridley, and J. Kroll, 2018: Causes and consequences of decreasing atmospheric organic aerosol in the United States. *Proc. Natl. Acad. Sci. USA*, **115**, 290–295, https://doi.org/10.1073/pnas.1700387115.

Rose, D., S. Gunthe, E. Mikhailov, G. Frank, U. Dusek, M. Andreae, and U. Pöschl, 2008: Calibration and measurement uncertainties of a continuous-flow cloud condensation nuclei counter (DMT-CCNC): CCN activation of ammonium

sulfate and sodium chloride aerosol particles in theory and experiment. *Atmos. Chem. Phys.*, **8**, 1153–1179, https://doi.org/10.5194/acp-8-1153-2008.

Samburova, V., A. Hallar, L. Mazzoleni, P. Saranjampour, D. Lowenthal, S. Kohl, and B. Zielinska, 2013: Composition of water-soluble organic carbon in non-urban atmospheric aerosol collected at the Storm Peak Laboratory. *Environ. Chem.*, **10**, 370–380, https://doi.org/10.1071/EN13079.

Saxena, P., and L. Hildemann, 1996: Water-soluble organics in atmospheric particles: A critical review of the literature and application of thermodynamics to identify candidate compounds. *J. Atmos. Chem.*, **24**, 57–109, https://doi.org/10.1007/BF00053823.

Schneider, J., S. Mertes, D. van Pinxteren, H. Herrmann, and S. Borrmann, 2017: Uptake of nitric acid, ammonia, and organics in orographic clouds: Mass spectrometric analyses of droplet residual and interstitial aerosol particles. *Atmos. Chem. Phys.*, **17**, 1571–1593, https://doi.org/10.5194/acp-17-1571-2017.

Schwab, J., and Coauthors, 2016a: Atmospheric chemistry measurements at Whiteface Mountain, NY: Cloud water chemistry, precipitation chemistry, and particulate matter. *Aerosol Air Qual. Res.*, **16**, 841–854, https://doi.org/10.4209/aaqr.2015.05.0344.

——, and Coauthors, 2016b: Atmospheric science research at Whiteface Mountain, NY: Site description and history. *Aerosol Air Qual. Res.*, **16**, 827–840, https://doi.org/10.4209/aaqr.2015.05.0343.

Seinfeld, J., and S. Pandis, 2016: *Atmospheric Chemistry and Physics: From Air Pollution to Climate Change.* John Wiley & Sons Inc., 1152 pp.

Shapiro, E., J. Szprengiel, N. Sareen, C. Jen, M. Giordano, and V. McNeill, 2009: Light-absorbing secondary organic material formed by glyoxal in aqueous aerosol mimics. *Atmos. Chem. Phys.*, **9**, 2289–2300, https://doi.org/10.5194/acp-9-2289-2009.

Shingler, T., and Coauthors, 2012: Characterisation and airborne deployment of a new counterflow virtual impactor inlet. *Atmos. Meas. Tech.*, **5**, 1259–1269, https://doi.org/10.5194/amt-5-1259-2012.

Stein, A., R. Draxler, G. Rolph, B. Stunder, M. Cohen, and F. Ngan, 2015: NOAA's HYSPLIT atmospheric transport and dispersion modeling system. *Bull. Amer. Meteor. Soc.*, **96**, 2059–2077, https://doi.org/10.1175/BAMS-D-14-00110.1.

Sullivan, A., R. Weber, A. Clements, J. Turner, M. Bae, and J. Shauer, 2004: A method for on-line measurement of water-soluble organic carbon in ambient aerosol particles: Results from an urban site. *Geophys. Res. Lett.*, **31**, L13105, https://doi.org/10.1029/2004GL019681.

——, and Coauthors, 2016: Evidence for ambient dark aqueous SOA formation in the Po Valley, Italy. *Atmos. Chem. Phys.*, **16**, 8095–8108, https://doi.org/10.5194/acp-16-8095-2016.

Sun, Y., Q. Zhang, C. Anastasio, and J. Sun, 2010: Insights into secondary organic aerosol formed via aqueous-phase reactions of phenolic compounds based on high resolution mass spectrometry. *Atmos. Chem. Phys.*, **10**, 4809–4822, https://doi.org/10.5194/acp-10-4809-2010.

Tan, Y., M. Perri, S. Seitzinger, and B. Turpin, 2009: Effects of precursor concentration and acidic sulfate in aqueous glyoxal–OH radical oxidation and implications for secondary organic aerosol. *Environ. Sci. Technol.*, **43**, 8105–8112, https://doi.org/10.1021/ES901742f.

——, A. Carlton, S. Seitzinger, and B. Turpin, 2010: SOA from methylglyoxal in clouds and wet aerosols: Measurement and prediction of key products. *Atmos. Environ.*, **44**, 5218–5226, https://doi.org/10.1016/j.atmosenv.2010.08.045.

Tilgner, A., B. Heinold, A. Nowak, and H. Herrmann, 2005: Meteorological characterisation of the FEBUKO hill cap cloud experiments, Part I: Synoptic characterisation of measurement periods. *Atmos. Environ.*, **39**, 4185–4194, https://doi.org/10.1016/J.ATMOSENV.2005.02.006.

——, and Coauthors, 2014: Comprehensive assessment of meteorological conditions and airflow connectivity during HCCT-2010. *Atmos. Chem. Phys.*, **14**, 9105–9128, https://doi.org/10.5194/acp-14-9105-2014.

Tong, H., and Coauthors, 2017: Reactive oxygen species formed in aqueous mixtures of secondary organic aerosols and mineral dust influencing cloud chemistry and public health in the Anthropocene. *Faraday Discuss.*, **200**, 251–270, https://doi.org/10.1039/C7FD00023E.

Torres, O., P. Bhartia, G. Taha, H. Jethva, and C. Ahn, 2018: Stratospheric injection of massive smoke plume from Canadian Boreal fires in 2017 as seen by DSCOVR-EPIC, CALIOP and OMPS-LP observations. *2018 AGU Fall Meeting*, Washington, DC, Amer. Geophys. Union, Abstract A41J-3092.

Tsui, W., J. Woo, and V. McNeill, 2019: Impact of aerosol-cloud cycling on aqueous secondary organic aerosol formation. *Atmosphere*, **10**, 666, https://doi.org/10.3390/ATMOS10110666.

van Pinxteren, D., and Coauthors, 2005: Schmücke hill cap cloud and valley stations aerosol characterisation during FEBUKO (II): Organic compounds. *Atmos. Environ.*, **39**, 4305–4320, https://doi.org/10.1016/j.atmosenv.2005.02.014.

——, and Coauthors, 2016: Cloud water composition during HCCT-2010: Scavenging efficiencies, solute concentrations, and droplet size dependence of inorganic ions and dissolved organic carbon. *Atmos. Chem. Phys.*, **16**, 3185–3205, https://doi.org/10.5194/acp-16-3185-2016.

Volkamer, R., and Coauthors, 2006: Secondary organic aerosol formation from anthropogenic air pollution: Rapid and higher than expected. *Geophys. Res. Lett.*, **33**, L17811, https://doi.org/10.1029/2006GL026899.

Weathers, K., and Coauthors, 1988: Cloudwater chemistry from ten sites in North America. *Environ. Sci. Technol.*, **22**, 1018–1026, https://doi.org/10.1021/es00174a004.

Williams, B., and Coauthors, 2014: The first combined thermal desorption aerosol gas chromatograph-aerosol mass spectrometer (TAG-AMG). *Aerosol Sci. Technol.*, **48**, 358–370, https://doi.org/10.1080/02786826.2013.875114.

Wobrock, W., and Coauthors, 1994: The Kleiner Feldberg cloud experiment 1990. An overview. *J. Atmos. Chem.*, **19**, 3–35, https://doi.org/10.1007/BF00696581.

Yin, B., Q. Min, M. Duan, M. Bartholomew, A. Vogelmann, and D. Turner, 2011: Retrievals of cloud optical depth and effective radius from thin-cloud rotating shadowband radiometer measurements. *J. Geophys. Res.*, **116**, D23208, https://doi.org/10.1029/2011JD016192.

Yu, L., J. Smith, A. Laskin, C. Anastasio, J. Laskin, and Q. Zhang, 2014: Chemical characterization of SOA formed from aqueous-phase reactions of phenols with the triplet excited state of carbonyl and hydroxyl radical. *Atmos. Chem. Phys.*, **14**, 13801–13816, https://doi.org/10.5194/acp-14-13801-2014.

——, ——, ——, K. George, C. Anastasio, J. Laskin, A. Dillner, and Q. Zhang, 2016: Molecular transformations of phenolic SOA during photochemical aging in the aqueous phase: Competition among oligomerization, functionalization, and fragmentation. *Atmos. Chem. Phys.*, **16**, 4511–4527, https://doi.org/10.5194/acp-16-4511-2016.

Zhang, G., and Coauthors, 2017: Insight into the in-cloud formation of oxalate based on in situ measurement by single particle mass spectrometry. *Atmos. Chem. Phys.*, **17**, 13891–13901, https://doi.org/10.5194/acp-17-13891-2017.

Zhang, J., S. Lance, R. Brandt, J. Marto, M. Ninneman, and J. Schwab, 2019: Observed below-cloud and cloud interstitial submicron aerosol chemical and physical properties at Whiteface Mountain, New York, during August 2017. *Earth Space Chem.*, **3**, 1438–1450, https://doi.org/10.1021/acsearthspacechem.9b00117.

Zhang, Q., M. Alfarra, D. Worsnop, J. Allan, H. Coe, M. Canagaratna, and J. Jimenez, 2005: Deconvolution and quantification of hydrocarbon-like and oxygenated organic aerosols based on aerosol mass spectrometry. *Environ. Sci. Technol.*, **39**, 4938–4952, https://doi.org/10.1021/es048568l.

——, and Coauthors, 2007: Ubiquity and dominance of oxygenated species in organic aerosols in anthropogenically-influenced Northern Hemisphere midlatitudes. *Geophys. Res. Lett.*, **34**, L13801, https://doi.org/10.1029/2007GL029979.

Zhang, X., and Coauthors, 2017: Highly oxygenated multifunctional compounds in α-pinene secondary organic aerosol. *Environ. Sci. Technol.*, **51**, 5932–5940, https://doi.org/10.1021/ACS.EST.6B06588.